KSHV lytic mRNA is efficiently translated in the absence of eIF4F

Eric S. Pringle [1, 2], Carolyn-Ann Robinson [3], Nicolas Crapoulet [4], Andrea L-A. Monjo [1], Katrina Bouzanis [1], Andrew M. Leidal [5], Stephen M. Lewis [1, 2, 4, 6, 7], Daniel Gaston [2, 8], James Uniacke [9], Craig McCormick [1, 2, *]

[1]Department of Microbiology & Immunology, Dalhousie University, 5850 College Street, Halifax NS, Canada B3H 4R2

[2]Beatrice Hunter Cancer Research Institute, 5850 College Street, Halifax NS Canada B3H 4R2

[3]Department of Microbiology, Immunology and Infectious Diseases, University of Calgary, Calgary AB, Canada T2N 4N1

[4]Atlantic Cancer Research Institute, 35 Providence Street, Moncton NB, Canada E1C 8X3

[5]Department of Pathology, 513 Parnassus Ave., University of California San Francisco, San Francisco CA, USA 94143

[6]Department of Chemistry and Biochemistry, Université de Moncton, Moncton NB, Canada E1A 3E9

[7]Department of Biology, University of New Brunswick, Saint John NB, Canada E2L 4L5

[8]Department of Pathology, Dalhousie University, 5850 University Avenue, Halifax NS, Canada B3H 4R2

[9]Department of Molecular and Cellular Biology, University of Guelph, 50 Stone Road E., Guelph ON, Canada N1G 2W1

[*]Corresponding author: C.M., craig.mccormick@dal.ca

Running Title: Translational efficiency of KSHV mRNA

Keywords: KSHV; mTORC1; translation initiation; polysomes; RNA-seq; translational efficiency; eIF4F; eIF4E2; eIF4G2; METTL3

ABSTRACT

Herpesvirus genomes are decoded by host RNA polymerase II, generating messenger ribonucleic acids (mRNAs) that are post-transcriptionally modified and exported to the cytoplasm. These viral mRNAs have 5′-m^7GTP caps and poly(A) tails that should permit assembly of canonical eIF4F cap-binding complexes to initiate protein synthesis. However, we have shown that chemical disruption of eIF4F does not impede KSHV lytic replication, suggesting that alternative translation initiation mechanisms support viral protein synthesis. Here, using polysome profiling analysis, we confirmed that eIF4F disassembly did not affect the efficient translation of viral mRNAs during lytic replication, whereas a large fraction of host mRNAs remained eIF4F-dependent. Lytic replication altered multiple host translation initiation factors (TIFs), causing caspase-dependent cleavage of eIF2α and eIF4G1 and decreasing levels of eIF4G2 and eIF4G3. Non-eIF4F TIFs NCBP1, eIF4E2 and eIF4G2 associated with actively translating messenger ribonucleoprotein (mRNP) complexes during KSHV lytic replication, but their depletion by RNA silencing did not affect virion production, suggesting that the virus does not exclusively rely on one of these alternative TIFs for efficient viral protein synthesis. METTL3, an N^6-methyladenosine (m6A) methyltransferase that modifies mRNAs and influences translational efficiency, was dispensable for early viral gene expression and genome replication but required for late gene expression and virion production. METTL3 was also subject to caspase-dependent degradation during lytic replication, suggesting that its positive effect on KSHV late gene expression may be indirect. Taken together, our findings reveal extensive remodelling of TIFs during lytic replication, which may help sustain efficient viral protein synthesis in the context of host shutoff.

IMPORTANCE

Viruses use host cell protein synthesis machinery to create viral proteins. Herpesviruses have evolved a variety of ways to gain control over this host machinery to ensure priority synthesis of viral proteins and diminished synthesis of host proteins with antiviral properties. We have shown that a herpesvirus called KSHV disrupts normal cellular control of protein synthesis. A host cell protein complex called eIF4F starts translation of most cellular mRNAs, but we observed it is dispensable for efficient synthesis of viral proteins. Several proteins involved in alternative modes of translation initiation were likewise dispensable. However, an enzyme called METTL3

63 that modifies mRNAs is required for efficient synthesis of certain late KSHV proteins and
64 productive infection. We observed caspase-dependent degradation of several host cell translation
65 initiation proteins during infection, suggesting that the virus alters pools of available factors to
66 favour efficient viral protein synthesis at the expense of host protein synthesis.
67

68 **INTRODUCTION**

69 All viruses use host translation machinery to create viral proteins. Most RNA viruses replicate in
70 the cytoplasm where they cannot access normal host mRNA processing machinery, so they must
71 encode their own proteins to transcribe and process viral mRNAs, while accessing host factors
72 that promote mRNA stability and enable efficient ribosome loading. Some RNA viruses have
73 structured motifs in 5' untranslated regions (UTRs) that directly recruit the small ribosomal
74 subunit with minimal involvement of host proteins (1). By contrast, DNA viruses, such as
75 herpesviruses, replicate in the nucleus where they can access the full complement of host
76 transcription machinery (2–4) Thus, herpesvirus mRNAs are transcribed by RNA polymerase II
77 (Pol II) and processed by enzymes that add 5' m^7GTP caps and 3' poly-adenylate (polyA) tails,
78 features that promote mRNA stability and provide access to the same cap-dependent translation-
79 initiation factors (TIF) employed by cellular mRNAs (3, 5).

80 Despite their strong resemblance to their host counterparts, herpesvirus mRNAs benefit
81 from several advantages that confer priority access to host translation machinery. During
82 Kaposi's sarcoma-associated herpesvirus (KSHV) latency, viral mRNAs are spliced by host
83 machinery (6), which promotes recruitment of the human transcription/export (hTREX) complex
84 that promotes mRNA stability and export to the cytoplasm, just as it does for host mRNAs. By
85 contrast, most lytic KSHV mRNAs are not spliced, and hTREX recruitment requires the viral
86 RNA-binding protein (RBP) ORF57, a homolog of HSV-1 ICP27, also known as mRNA
87 transcript accumulation (Mta) (7–9). ORF57 RNA-binding determinants and interplay with other
88 components of the host mRNA processing machinery remain poorly defined, but it clearly
89 enables efficient constitutive export of unspliced viral mRNAs, providing a selective advantage
90 over host mRNAs that require splicing and are subject to stress-regulated regulation of the
91 splicing reaction (8). In the cytoplasm, ORF57 remains associated with these viral messenger
92 ribonucleoprotein (mRNP) complexes following translation initiation where it supports
93 translation of non-spliced viral mRNA (7). ORF57 is also sufficient to inhibit the formation of

94 cytoplasmic stress granules (SGs) that normally form in response to the accumulation of
95 translationally stalled mRNP complexes (10), suggesting that it may be able to sustain ongoing
96 protein synthesis during times of stress that would normally prohibit it. In addition to bypassing
97 canonical splicing-dependent mRNA export mechanisms, several studies have reported extensive
98 N^6-methyladenosine (m^6A) modification of KSHV mRNAs including mRNAs encoding the
99 immediate-early gene product RTA (11–14). m^6A is co-transcriptionally deposited on mRNA by
100 the m^6A "writer" enzyme, METTL3 (15–17). m^6A modifications have a variety of effects on can
101 regulate splicing, stability, secondary structure, accumulation in RNA condensates, and
102 translation (12, 15, 18–22). These effects are promoted by m^6A "reader" proteins YTH-domain
103 and Tudor family of RNA-binding proteins (14, 23, 24).
104 In typical cell culture experiments (normoxia, rich culture media), approximately two-
105 thirds of global protein synthesis requires eIF4F, a protein complex comprising the m^7GTP cap-
106 binding protein eIF4E1, the scaffolding protein eIF4G1 (or eIF4G3), and the eIF4A RNA
107 helicase (1, 25–27). After the cap is bound by eIF4E1, eIF4G1/3 recruits eIF3 and the small
108 ribosomal subunit to initiate scanning for the start codon. eIF4A with its cofactors eIF4B and
109 eIF4H reduce secondary structure in the 5'UTR to facilitate this process (26, 27). In response to
110 nutrients and growth signals, mechanistic target of rapamycin complex 1 (mTORC1) regulates
111 translation initiation by promoting assembly of the eIF4F initiation complex. When
112 unphosphorylated, repressive 4E-BP1 proteins bind to the eIF4E cap-binding protein and prevent
113 recruitment the eIF4G1/3 scaffolding protein. mTORC1-mediated phosphorylation of 4E-BP1
114 liberates eIF4E and enables eIF4F assembly and subsequent recruitment of the eIF3 complex and
115 the small ribosomal subunit (1, 2, 28). mTORC1 inhibition causes widespread decreases in
116 protein synthesis, but transcripts bearing 5' terminal oligopyrimidine (TOP) sequences (25) or
117 pyrimidine-rich translational element (PRTE) sequences (29) at their 5′ ends are especially
118 sensitive to mTORC1. These sequences allow for association of the cap-binding protein LARP1,
119 which sequesters the cap and limits further cap-dependent initiation (30–32). By contrast, eIF4F-
120 independent protein synthesis mechanisms remain poorly understood, and the field is only
121 beginning to identify and characterize TIFs involved in these processes (18, 33–35).
122 Herpesviruses from all subfamilies (alpha-, beta-, and gammaherpesviruses) have been
123 shown to activate mTORC1 during lytic replication (36–39), but paradoxically, viral protein
124 synthesis and virion production are largely unaffected by mTORC1 inhibition (38, 40, 41). We

125 and others have shown that eIF4F assembles and remains sensitive to the mTORC1 active-site
126 inhibitor Torin throughout the KSHV lytic replication cycle (38, 39, 42). However, mTORC1
127 activity was dispensable for KSHV protein synthesis and genome replication, and only modestly
128 inhibited virion production (38). These findings suggest that translation of KSHV mRNAs has a
129 reduced dependence on eIF4F.
130 To better understand the determinants of KSHV protein synthesis in the context of lytic
131 replication, we used polysome profiling to measure translational efficiency (TE) of viral
132 mRNAs. We observed that viral mRNAs readily persist in polysomes in the absence of eIF4F
133 components eIF4G1 and eIF4G3. This finding is consistent with previous observations of robust
134 translation of human cytomegalovirus (HCMV) mRNAs despite eIF4F disassembly (40) and
135 suggests that non-eIF4F translation initiation mechanisms are likely sufficient to support
136 synthesis of herpesvirus proteins. We found that pro-viral caspase activation during lytic
137 replication (43) causes cleavage of several host TIFs, but this has no effect on rates of global
138 protein synthesis in the low translation environment of lytic replication. We tested the
139 contribution of TIFs that participate in non-eIF4F translation initiation mechanisms and found
140 that NCBP1, eIF4E2, and eIF4G2 were dispensable for virion production. However, METTL3
141 silencing, which would result in defects in m^6A-dependent translation (18, 19, 44–46), caused a
142 ten-fold loss in virion production without affecting viral genome replication. These findings
143 suggest that viral mRNAs are efficiently recruited to ribosomes in the low-translation
144 environment of lytic replication despite significant changes in available translation initiation
145 factors.
146
147 **RESULTS**
148 **Translation of KSHV lytic mRNAs are resistant to mTOR inhibition**. Our group and others
149 previously reported that eIF4F assembles during KSHV latency and lytic replication and remains
150 under strict regulation by mTORC1 and 4E-BP1 (38, 39). Here, we used polysome profiling to
151 measure how eIF4F disruption affected translational efficiency (TE) of viral mRNAs.
152 Physiologic mTORC1 activity is regulated by amino acid abundance, but mTORC1 is readily
153 inhibited by several drugs, including the potent active site inhibitor Torin 1 (hereafter known as
154 Torin) (42). We observed that Torin treatment of uninfected iSLK cells for 2 h prior to harvest
155 caused dephosphorylation of ribosomal protein S6 and 4E-BP1 as expected, which was likewise

156 evident in latently KSHV-infected iSLK.219 cells, or cells which had been treated with
157 doxycycline (dox) for 48 h to activate the lytic cycle (Fig. 1A). In these experiments, we
158 reactivated iSLK.219 cells with doxycycline only; we omitted the HDAC inhibitor sodium
159 butyrate that is commonly used to promote lytic reactivation in an attempt to limit potentially
160 confounding effects of epigenetic regulation of transcription by histone acetylation. Under these
161 conditions, many of the iSLK.219 cells either fail to reactivate or undergo abortive replication.
162 Nevertheless, it remains clear that mTORC1 regulation of canonical target proteins S6 and 4E-
163 BP1 remain largely intact during latent and lytic phases of KSHV replication (Fig. 1A).
164 We observed that Torin treatment of uninfected iSLK cells shifted mRNAs from
165 efficiently translated heavy polysomes to poorly translated sub-polysomal fractions (Fig. 1B)
166 consistent with studies of other cell types (25, 40). Latently infected iSLK.219 cells treated with
167 Torin displayed a similar shift of mRNA into sub-polysomal fractions. After 48 h of dox
168 treatment, the heavy polysomes were depleted, likely due to host shutoff in lytic cells (47) and
169 the depletion of the media over the incubation time in cells in which KSHV failed to reactivate
170 from latency (Fig. 1B). In this population, Torin treatment further depleted the heavy polysome
171 fractions, although the effects were modest, likely due to the pre-existing low translation
172 environment in these cells.
173 To measure the effects of mTORC1 inhibition on the TE of viral and host mRNAs during
174 the KSHV lytic cycle, we isolated RNA from polysome fractions from Torin- and vehicle-treated
175 48 h post-dox cells (Fig. 1B, bottom panel), and processed it for RNA sequencing. We assessed
176 TE by division of the number of reads isolated from the polysomes compared to the reads found
177 in the total RNA fraction (# of reads polysome / # of reads total). The abundance of KSHV
178 transcripts differed by as much as 100,000-fold with ten-fold more of the non-coding PAN RNA
179 than the next most abundant RNA. The most abundant protein-coding viral mRNAs encode the
180 ORF59 processivity factor, Kaposin (K12), vIL-6 (K2), and the viral dUTPase-like gene ORF11
181 (Fig. 2A) (3, 48). The TE of viral mRNAs appeared to be generally similar to cellular mRNAs,
182 although assessment of cellular mRNAs is complicated in this system because they are derived
183 from a mixed population of lytically-replicating cells and non-reactivated cells. Consistent with
184 the literature, we observed alterations in TE of cellular mRNAs in the presence of Torin, with
185 populations of mRNAs displaying increased or decreased TE (Fig. 2B). We scored the difference
186 in translational efficiencies by using a sliding-window to calculate a Z-score of each detected

187 transcript compared to the surrounding 200 transcripts of similar abundance as measured by
188 count per million (CPM) (49, 50). The ΔTE of the majority of viral mRNAs (~90%) was not
189 inhibited or enhanced by a conservative Z-score of 1 (Fig. 2B, Z-score within 1 SD of the mean
190 in blue, Z-score > 1 SD of the mean in red), suggesting that the TE of viral transcripts is likely
191 not regulated by the mTORC1/4E-BP/eIF4F axis.
192 We analysed transcripts with a greater than 1.5-fold change in TE using the Panther GO-
193 Slim Molecular Function analysis (Fig. 2C). Both ribosomal structural proteins and TIF were
194 over-represented in host cell transcripts with reduced TE following Torin treatment, consistent
195 with previous studies (25, 29), which suggests that TOP-containing transcripts are regulated by
196 mTORC1 as expected during KSHV lytic replication. By contrast, host transcripts with increased
197 TE following Torin treatment did not group into any clear molecular function. Because we
198 mapped RNA-seq reads by individual transcripts rather than genes, we could detect a slight yet
199 significant ($p<0.0001$) enrichment of normally labile pseudogene mRNAs in high TE groups,
200 and their corresponding diminishment in low TE groups (Fig. 2D). Rather than reflecting
201 changes in TE of pseudogene mRNAs, we suspect this result could be explained by
202 accumulation of ribosomes due to halted elongation while the mRNA is processed by nonsense-
203 mediated decay (NMD) and other ribosomal quality control processes (reviewed in (51)).
204
205 **eIF4F disassembly does not deplete viral mRNAs from polysomes.** We corroborated our
206 findings of eIF4F-independent efficient translation of viral mRNAs in the primary effusion
207 lymphoma (PEL)-derived TREx-BCBL1-RTA cell model; these cells reactivate efficiently in
208 response to dox treatment compared to iSLK.219 cells, which helps reduce confounding effects
209 of failed lytic reactivation. Furthermore, the lytic cycle proceeds more quickly in TREx-BCBL1-
210 RTA cells, with robust virion production achieved by 48 hpi (38). TREx-BCBL1-RTA cells
211 were reactivated with dox for 24 h and treated with Torin or vehicle control for the final 2 h or
212 replication before lysis and polysome profiling. We isolated mRNA from sub-polysome, light
213 polysome, and heavy polysome fractions and performed RT-qPCR on select mRNAs to
214 determine their distribution across the polysome profile as an alternative measure of TE (52).
215 Consistent with observations in the iSLK.219 cells (Fig. 1B), Torin treatment of lytic TREx-
216 BCBL1-RTA cells caused a moderate shift of bulk mRNA from polysomes to sub-polysomal
217 fractions (Fig. 3A). We used RT-qPCR to measure the distribution of cellular and viral mRNAs

218 in polysomes or lighter fractions. Torin treatment caused shifted β-actin mRNA from heavy
219 polysomes to monosome and sub-monosome fractions (Fig. 3B). However, a significant
220 proportion of translating β-actin mRNA remained in the polysome fractions despite Torin
221 treatment. By contrast, Torin treatment caused the TOP-mRNAs encoding Rps20 and RACK1 to
222 completely shift from polysome fractions to sub-polysome and monosome fractions. This is
223 consistent with the RNA-seq analysis and confirms that TOP mRNAs remain susceptible to
224 eIF4F disassembly during the lytic cycle.
225 Historically, the contribution of monosomes to global protein synthesis has been
226 overlooked, but recent ribosomal foot-printing studies have revealed that monosomes contain
227 translationally active mRNAs, notably including unusual mRNAs with short open reading frames
228 (ORFs), up-stream ORFs (uORFs), or low initiation rates (53). We observed that mRNAs
229 encoding VEGF-A and IL6, two cytokines with significant contributions to KSHV pathogenesis
230 (54–56), were abundant in monosome fractions despite abundant VEGF-A and IL6 in
231 supernatants from lytic TREx-BCBL1-RTA cells (38); this suggests that monosomes may make
232 significant contributions to translation of these cytokines during lytic replication. We also
233 analyzed the polysomal distribution of viral mRNAs from all three transcriptional classes: Latent
234 (LANA, Kaposin), early (ORF11, ORF45, vIL-6), and late (K8.1, ORF26, ORF65). The TE of
235 all viral mRNAs tested generally seemed to resist Torin inhibition, but a slight shift towards the
236 sub-polysomal fractions can be detected (Fig. 4B). Combined with our previous assessments in
237 iSLK.219 cells (Fig. 2B), these findings suggest that during KSHV lytic replication, host cell
238 transcripts are regulated by the mTORC1-4EBP1-eIF4F signalling axis as expected, whereas
239 viral transcripts are not.
240
241 **Translation initiation factors eIF2α and eIF4G1 are cleaved by caspases during lytic**
242 **replication.** Activation of pro-apoptotic caspase-3 and caspase-8 during KSHV lytic replication
243 limit interferon (IFN) production and promote virus replication (43). Paradoxically, this caspase
244 activation does not contribute to apoptosis, likely due to the actions of viral anti-apoptotic
245 proteins vFLIP, vBcl2, and K7 (57–59). In uninfected cells, caspases also cleave the translation
246 initiation factors (TIF) eIF2α and eIF4G1, which may limit protein synthesis during apoptosis
247 (60, 61). We hypothesized that caspase-dependent cleavage of TIFs might contribute to host
248 shutoff and eIF4F-independent translation of KSHV mRNAs during the lytic cycle. Indeed,

249 TREx-BCBL1-RTA cells reactivated with dox displayed a decrease in total eIF4G1 abundance
250 consistent with caspase-3 activation and eIF4G1 cleavage during lytic replication (Fig. 4A; (62)).
251 We also observed faster-migrating protein species that reacted with anti-eIF2α, -eIF4G2, and -
252 ORF57 antibodies, all of which were previously described caspase substrates (60, 63, 64). To
253 confirm caspase activation during KSHV lytic replication, we reactivated TREx-BCBL1-RTA
254 cells with dox in the presence of a pan-caspase inhibitor IDN-6556 or vehicle control; we
255 observed the accumulation of cleaved caspase-3 over a 48 h time course, which was sensitive to
256 IDN-6556 (Fig. 4B). Caspase inhibition also prevented the degradation of eIF4G1 and cleavage
257 of eIF2α and ORF57. Loss of ORF57 cleavage with IDN-6556 also supports the notion that
258 caspases are active in lytic cells and not only in those latently infected or undergoing abortive
259 infection. We measured global protein synthesis using a ribopuromycinylation assay whereby
260 puromycin is incorporated into elongating polypeptides where it can be subsequently detected
261 using an anti-puromycin antibody (65). Similar to previous reports, we observed a clear decrease
262 in global protein synthesis during KSHV lytic replication (38, 66, 67) which was unaffected by
263 caspase inhibition (Figs. 4B, 4C). We conclude that TIF degradation by caspases does not
264 contribute to host shutoff.
265
266 **eIF4F disassembly selectively displaces host translation initiation factors from polysomes**
267 **during KSHV latency and lytic replication.** Considering the evidence for eIF4F-independent
268 translation of KSHV mRNAs and caspase-mediated TIF remodeling, we reasoned that
269 alternative TIFs could play an important role in supporting efficient synthesis of lytic proteins.
270 As a first step in this investigation, we profiled TIF recruitment to polysomes during lytic
271 replication and whether these components could be displaced by mTORC1 inhibition. TREx-
272 BCBL1-RTA cells were once again reactivated with dox for 22 h and treated with Torin for 2 h
273 prior to lysis and polysome profiling. Consistent with our previous findings, mTORC1 inhibition
274 caused dephosphorylation of canonical substrates S6 and 4E-BP1, both during latency and lytic
275 replication (Fig. 5A). Once again, lytic replication in TREx-BCBL1-RTA cells caused a bulk
276 shift of mRNAs from polysomes to sub-polysomal fractions, with the residual translation
277 remaining sensitive to mTORC1 inhibition and eIF4F disassembly (Fig. 5B). We assessed the
278 proteins associated with polysomes by immunoblotting proteins harvested from gradient
279 fractions using a low-salt lysis buffer to aid retention of eIF4F components and other RBPs,

280 consistent with previous ribosome isolation protocols (68, 69). Fractions were isolated from the
281 40S, 60S, and 80S sub-polysomal peaks, as well as light and heavy polysomes; RNA and
282 associated proteins were precipitated using ethanol and a glycogen co-precipitant.
283 Additional m^7GTP cap-binding proteins beyond the canonical eIF4E1 protein include
284 nuclear cap-binding protein subunit 1 (NCBP1), which promotes pioneer translation on newly
285 transcribed mRNA (34), and eIF4E2, which contributes to global protein synthesis at physiologic
286 oxygen tension and is strictly required for hypoxic translation (33). We observed that eIF4E1,
287 eIF4E2 and NCBP1 associated with polysomes in all conditions tested, as expected (Fig. 5C).
288 Torin treatment caused a progressive loss of eIF4F components eIF4G1 and eIF4G3 from
289 polysome fractions (Fig. 5C), consistent with displacement of eIF4G from the eIF4F complex by
290 hypophosphorylated 4E-BP1 (Fig. 5A). However, eIF4G2, which was found primarily in the 80S
291 monosome peak and sub-monosomal fractions, was unaffected by mTORC1 inhibition. eIF4G2
292 may function as an eIF4G1-like factor for cap-dependent translation of mRNA that directly bind
293 to eIF3 protein eIF3d (70). We noted a striking accumulation of a faster migrating species of
294 eIF4G1 in lytic cells that matches a previously reported 120 kDa caspase-3 cleavage fragment
295 (62), consistent with our observation of eIF4G1 cleavage by caspases in these cells (Fig. 4B).
296 Interestingly, this 120 kDa eIF4G1 fragment remained associated with polysomes in Torin-
297 treated cells, whereas full-length eIF4G1 is lost (Fig. 5C). Hyper-phosphorylated 4E-BP1 was
298 associated with polysomes in vehicle-treated samples, consistent with previous reports of 4E-
299 binding proteins co-sedimenting with polysome fractions (71). Hypophosphorylated 4E-BP1 was
300 found in sub-polysomal fractions of Torin-treated cells in both the latent and lytic cell
301 populations. This data is consistent with destabilization of eIF4G-eIF4E complexes upon cap
302 binding and dynamic disassembly of eIF4F after initiation, as hypothesized by Merrick (2015)
303 (27). Finally, consistent with previous reports (7), the lytic KSHV mRNA binding protein
304 ORF57 was associated with mRNAs in polysomes, and remained associated following mTORC1
305 inhibition (Fig. 5C). Taken together, these findings indicate that even though mTORC1 is active
306 and eIF4F is assembled during lytic replication, viral mRNAs can be efficiently translated
307 despite eIF4F depletion. Moreover, these experiments provide evidence for remodeling of
308 polysome- and monosome-associated mRNP complexes during lytic replication.
309 We next used RNA silencing to test the potential contributions of eIF4E2, eIF4G2, and
310 NCBP1 on virus replication, all of which could potentially support translation of viral mRNA

311 either constitutively or when eIF4F is limited. However, knockdown of these factors had no
312 effect on virus replication in the presence of absence of mTORC1 inhibition (Fig 6), consistent
313 with our previous observations that KSHV virion production has a limited requirement for
314 mTORC1 activity once early gene expression is established (38). We further tested the
315 requirement of eIF4E2 on KSHV replication during hypoxia. During hypoxia, regulated in
316 development and DNA damage response 1 (REDD1) normally promotes the inhibitory activity
317 the tuberous sclerosis complex (TSC) on mTORC1 (72), an action which could potentially be
318 antagonized by viral mTORC1-activating proteins. However, we observed that KSHV replicated
319 equally well in TREx-BCBL1-RTA cells in hypoxic conditions as it did in normoxia, and
320 eIF4E2 was dispensable, even when eIF4F was depleted (Fig. 6, top panels). This suggests that
321 KSHV is competent to complete its replication cycle during hypoxia and able to utilize an
322 eIF4E2- or an $eIF4F_H$-independent mechanism to support viral protein synthesis.
323
324 **METTL3 is required for virion synthesis but not genome replication.** N^6-methyladenosine
325 modification (m^6A) of RNA can stimulate mRNA translation by either recruiting eIF3 and the
326 small ribosomal subunit directly, or by the actions of m^6A reader proteins (18, 19, 44). Many
327 KSHV mRNAs are modified with m^6A and these modifications likely affect the fate of transcript
328 (11–14). The m^6A methyltransferase METTL3 and the m^6A reader YTHDC2 have been shown
329 to affect KSHV virion production, but with conflicting results in different systems (11, 13). We
330 found that METTL3 protein levels were reduced by 24 hpi in TREx-BCBL1-RTA cells (Fig.
331 7A). However, despite being reduced at the protein level during lytic replication, RNA silencing
332 of METTL3 diminished virion output by 10-fold (Fig. 7B). Viral genome replication was
333 unperturbed by METTL3 silencing (Fig. 7C), but accumulation of early proteins ORF45 and
334 ORF17 and the late protein ORF65 were disrupted. ORF57 accumulates normally when
335 METTL3 is absent, suggesting that m^6A is not required for translation of ORF57. Similarly,
336 ORF59, which requires ORF57 binding for mRNA export (73, 74), accumulates normally in
337 METTL3 knockdown, suggesting that m^6A is not required for ORF57 association with mRNA
338 (Fig. 7A). Thus, in our hands, METTL3 is required for efficient synthesis of certain KSHV
339 proteins and virion production in the TREx-BCBL1-RTA cell system.
340 In the course of studying the effects of m^6A RNA modifications during KSHV infection,
341 Hesser et al., (2018) (13) and Tan et al., (2017) (11) used the histone deacetylase (HDAC)

342 inhibitor sodium butyrate (NaB) to enhance lytic reactivation in iSLK.219 cells; Hesser et al.,
343 (2018) (13) also used the phorbol ester TPA in m^6A studies using TREx-BCBL1-RTA cells for
344 similar reasons. In our experiments, we exclusively used doxycycline to reactivate the TREx-
345 BCBL1-RTA cells in an attempt to eliminate broad confounding effects of HDAC inhibitors and
346 phorbol esters. We reactivated TREx-BCBL1-RTA cells and iSLK.219 cells with dox in similar
347 conditions and confirmed a decrease in METTL3 abundance (Fig. 8A, 8B). Because the
348 immediate early KSHV lytic switch protein RTA is a SUMO-dependent E3 ubiquitin ligase
349 (STUbL), and METTL3 has been reported to be sumoylated (75, 76), we hypothesized that RTA
350 may promote proteasome-dependent degradation of METTL3. We tested this hypothesis using
351 parental iSLK cells that express RTA from a dox-inducible promoter but lack KSHV episomes.
352 Treatment of iSLK cells with dox caused RTA accumulation but had no effect on METTL3
353 protein levels (Fig. 8C). Furthermore, inhibiting proteasome function with MG132 increased
354 levels of RTA (indicating that the proteasome controls RTA protein turnover), but had no effect
355 on METTL3 protein levels in the presence or absence of RTA, demonstrating that METTL3 is
356 not constitutively degraded by the proteosome. By contrast, treatment of TREx-BCBL1-RTA
357 cells with the caspase inhibitor IDN-6556 sustained METTL3 protein levels at later stages of
358 lytic replication (Fig. 8D), which indicates that METTL3 is another substrate for caspase-
359 mediated cleavage during KSHV lytic replication.
360

361 **DISCUSSION**

362 KSHV mRNAs broadly resemble their cellular counterparts which should allow their
363 recruitment to ribosomes in an eIF4F-dependent manner. Here, we demonstrate that activation of
364 caspases during lytic replication degrades TIFs, yet this has no effect on protein synthesis after
365 host shutoff. The remaining eIF4G1 and eIF4G3 are effectively recruited to polysomes in an
366 mTORC1- and eIF4F-dependent manner. These heavily-translated mRNPs contain viral mRNA,
367 which remain in these fractions when eIF4F is depleted, suggesting that viral mRNAs do not
368 require eIF4F for efficient translation initiation. These observations are consistent with reports
369 from Lenarcic, et. al. (2014)(40), who demonstrated that mTORC1 is dispensable for HCMV late
370 protein synthesis and that Torin had little effect on TE of viral mRNAs. They also support our
371 previous findings that eIF4F disassembly does not impede KSHV replication and virion
372 production (38). Together, these observations suggest that resistance to eIF4F loss might be a

373 general feature of herpesvirus translation, even for viruses like HCMV that do not shut off host
374 gene expression. Moreover, our study indicates that mTORC1 and eIF4F maintain broad roles in
375 global translation regulation during KSHV lytic replication. Torin treatment depletes heavy
376 polysomes during lytic replication and shifts TOP-containing mRNAs encoding ribosomal
377 proteins and TIFs into sub-polysomal fractions. The most recent and thorough efforts to map
378 KSHV mRNA 5'-ends have not identified any TOP sequences (3, 5), which is consistent with
379 the idea that they could be efficiently translated despite mTORC1 inhibition.
380 Our polysome RNA-Seq analysis was restricted to heavy translating polysomes, but there
381 is emerging evidence that light polysomes and monosomes also make important contributions to
382 bulk protein synthesis (53, 77). While we could detect almost the entire viral transcriptome in
383 heavy polysome fractions, subsequent RT-qPCR measurements of select viral transcripts
384 revealed broad distribution across gradient fractions. Two notable exceptions were the
385 K12/Kaposin and LANA mRNAs, which were largely restricted to sub-polysomal fractions.
386 Both of these transcripts are spliced and encode multiple proteins via complex translational
387 programs that include leaky ribosomal scanning mechanisms of initiation (78, 79). They also
388 have long stretches of repeats that may impede efficient translation. For example, polyproline
389 motifs are slowly decoded by elongating ribosomes (80), and protein products of Kaposin
390 mRNAs feature numerous polyproline motifs (78). We speculate that preponderance of Kaposin
391 mRNAs in sub-polysome fractions could result from close proximity of polyproline-encoding
392 sequences to the several start codons on this mRNA, which could slow elongating ribosomes and
393 prevent or slow assembly of subsequent 80S complexes. The emerging role of monosome
394 translation in controlling the synthesis of highly regulated proteins should be considered in future
395 investigations of KSHV lytic gene expression.
396 Several studies have reported m^6A modification of KSHV mRNA, and m^6A modification
397 of RTA is required for proper splicing and stability (11–14). However, the precise roles for m^6A
398 modifications and m^6A reader proteins in the biogenesis and fate of KSHV mRNA other then
399 RTA remain to be discovered and may be dependent on cell type and different chemical stimuli
400 of lytic reactivation (13). N^6-methyladenosine (m^6A) dependent translation initiation has been
401 shown to contribute to residual translation following eIF4F disassembly in normoxia (19).
402 Unlike HCMV, we found that METTL3 is degraded by caspases during KSHV lytic replication
403 (81, 82). While this may preclude a significant role for m^6A modification as a global mechanism

404 of translation of viral mRNA, this modification has nevertheless been found to be widely
405 distributed across the genome (14). The effects of m^6A on virus titer might largely be explained
406 by a Type-I IFN response. Loss of m^6A marks on IFN-β mRNA promotes stabilization of the
407 transcript and leads to the accumulation of ISGs (81, 82). Additionally, we expect the wide
408 effects of METTL3 depletion on global transcription (83) likely have pleiotropic effects on
409 normal viral replication.
410 During Torin treatment, both the TOP-containing transcript Rps20 and the non-TOP -β-
411 actin transcript were depleted from polysome fractions that retained viral mRNA. In these same
412 fractions eIF4G1 and eIFG3 are also lost, but ORF57 is retained. ORF57 and related herpesvirus
413 homologues (EBV EB2 and HSV1/2 ICP27) have previously been shown to interact with
414 initiation factors, and can be found in polysomes (84, 85). In our experiments, loss of eIF4G
415 from polysomes with Torin treatment suggested that ORF57-dependent recruitment of eIF4G to
416 viral mRNA was not required for their translation, yet ORF57 is clearly present in the same
417 fractions as viral mRNA and is not displaced with eIF4F loss. This data suggests that while
418 mTORC1 is active during KSHV lytic, it is not required for the translation of viral mRNA.
419 While eIF4F is assembled during lytic replication, it is not required for the association of viral
420 mRNA with the polysomes. Alternative translation initiation factors, including eIF4E2, eIF4G2,
421 NCBP1, and eIF3d are also not required for virion production. Similarly, m^6A is not required for
422 the translation of ORF57 mRNA. However, ORF57 remains associated with the polysomes in
423 the absence of eIF4F. It is possible that ORF57, or other viral factors are required for KSHV
424 translation initiation, but the complement of host and viral proteins associating with translating
425 mRNA during lytic replication is unknown.
426
427 **METHODS**
428 **Cell culture and inhibitors.** TREx-BCBL1-RTA cells (86) were cultured in RPMI*1640
429 supplemented with 10% vol/vol heat-inactivated fetal bovine serum (Gibco), 5 mM L-glutamine,
430 and 50 μM β-mercaptoethanol. 293T cells, iSLK and iSLK.219 cells (a kind gift from Don
431 Ganem, (87)) were cultured in DMEM with 10% FBS, 5 mM L-Glutamine. Cells were
432 maintained at $37^{O}C$ at 5% CO2 using standards. All cells were maintained in 100 I/U of both
433 penicillin and streptomycin. iSLK.219 cells were cultured with 10 mM puromycin
434 (ThermoFisher Scientific) to maintain episome copy number of rKSHV.219. Puromycin was

435 omitted from cells seeded for experiments. Expression of the RTA transgene and lytic
436 reactivation in both the TREx-BCBL1-RTA and iSLK.219 was stimulated by treating the cells
437 with 1 µg/mL doxycycline. For hypoxia experiments, cells were placed in a Hypoxia Incubation
438 Chamber (StemCell); the chamber was purged with nitrogen at 2 psi for 5 min prior to sealing.
439 15 mM HEPES was added to the media in all hypoxia experiments to maintain media pH.
440 mTORC1 was inactivated by addition of 250 nM Torin (42) (Toronto Chemicals) in 0.1%
441 vol/vol DMSO. Caspases were inhibited with 10 µM IDN-6556 (Selleckchem) in 0.1% vol/vol
442 DMSO as described in (43).
443
444 **Western blotting.** TREx-BCBL1-RTA suspension cultures were collected by centrifugation at
445 1,500 x *g*, washed with ice-cold PBS, pelleted again, then lysed in 2x Laemmli buffer (4%
446 [wt/vol] sodium dodecyl sulfate [SDS], 20% [vol/vol] glycerol, 120 mM Tris-HCl [pH 6.8]).
447 iSLK and iSLK.219 cells were washed once with ice-cold PBS then lysed with 2x Laemmli
448 buffer directly in the well. DNA was sheared by repeated pipetting with a fine-gauge needle
449 before 100 mM dithiothreitol (DTT) addition and boiling at 95ºC for 5 min. Samples were stored
450 at -20ºC until analysis. Total protein concentration was determined by DC protein assay (Bio-
451 Rad) and equal quantities were loaded in each SDS-PAGE gel. Gels were transferred using to
452 polyvinylidene difluoride (PVDF) membranes (Bio-Rad) with the Trans-Blot Turbo transfer
453 apparatus (Bio-Rad). Membranes were blocked with 5% bovine serum albumin TBS-T (Tris-
454 buffered saline, 0.1% [vol/vol] Tween) before probing overnight at 4ºC with the following
455 antibodies: 4E-BP1 (Cell signaling technologies [CST] #9644), β-actin (CST #5125 or CST
456 #4970), cleaved caspase 3 (CST #9664), eIF2α (CST #9722), eIF4E1 (#2067), eIF4E2 (GeneTex
457 GTX103977), eIF4G1 (CST #2858), eIF4G2 (CST #5169), eIF4G3 (GeneTex GTX118109),
458 METTL3 (CST #96391), myc (CST #2276), NCBP1 (Abcam ab42389), Rps6 (S6; CST #2217)
459 phosphoSer235/6-Rps6 (CST #4858), ORF45 (ThermoFisher MA5-14769), ORF57 (Santa Cruz
460 Biotechnologies sc-135746), Kaposin (a kind gift from Don Ganem), LANA (a kind gift of Don
461 Ganem), RTA (a kind gift from David Lukac), ORF65 (a kind gift S.-J. Gao), ORF17 (a kind gift
462 from Charles Craik). Secondary antibodies HRP-conjugated for mouse (CST 7076) or rabbit
463 (CST 7074) were used with Clarity-ECL chemiluminescence reagent (Bio-Rad) for detection.
464 All blots were imaged on a Bio-Rad ChemiDoc-Touch system. Molecular weights were
465 determined using protein standards (New England Biolabs P7712, or P7719). Puromycin

466 incorporation assays were performed essentially as described in (38). Briefly, TREx-BCBL1-
467 RTA cells were treated with 10 µg/mL puromycin 10 min prior to harvest as described above.
468 Western blots for puromycin were run on 12% TGX Stain-Free FastCast acrylamide (Bio-Rad)
469 according to the manufacturer's instructions. Puromycin incorporation was detected using an
470 anti-puromycin antibody (EMD Millipore MABE43). For quantitative analysis, puromycin
471 signal was compared to the Stain-Free total protein signal.
472
473 **Polysome Isolation.** Polysomes were isolated by ultracentrifugation of cytosolic lysate through a
474 7-47% wt/vol linear sucrose gradient in high salt (20 mM Tris HCl, 300 mM NaCl, 25 mM
475 $MgCl_2$ in DEPC-treated or nuclease-free water) or low salt (15 mM Tris HCl, 50 mM KCl, 10
476 mM $MgCl_2$) lysis buffer with RNAse and protease inhibitors, as described in (52). High salt
477 conditions were used to isolate RNA from gradients and low salt conditions were used for
478 isolating proteins. Gradients were prepared using manufactures' settings on a Gradient Master
479 108 (Biocomp). For each gradient, ~8 x 10^6 iSLK.219 or 1.3 x 10^7 TREx-BCBL-RTA cells were
480 seed. Cells treated with 100 µg/mL cycloheximide (CHX, Acros Organics or Sigma) for three
481 min prior to harvest. Cells were washed with ice-cold PBS and scraped in a tube containing the
482 spent media and PBS wash. The cells were pelleted by centrifugation for 5 min at 500 x *g* and
483 washed again with ice-cold PBS. Cell pellets were resuspended in lysis buffer (high or low salt
484 buffer, with 1% v/v Triton X-100, 400 units/ml RNAseOUT (Invitrogen), 100 µg/mL CHX, and
485 protease and phosphatase inhibitors) for 10 min on ice. Lysate was centrifuged for 10 min at
486 2,300 x *g* the supernatant was transferred to a new tube and centrifuged for 10 min at 15,000 x *g*.
487 The supernatant was overlaid on sucrose gradients. Gradients were centrifuged at 39,000 rpm for
488 90 min on a SW-41 rotor. The bottom of the centrifuge tube was punctured, and 60% wt/vol
489 sucrose was underlain by syringe pump in order to collect 500 µL or 1 mL fractions from the top
490 of the gradient with simultaneous A_{260} measurement using a UA-6 detector (Brandel, MD).
491 Polysome sedimentation graphs were generated with Prism8 (GraphPad).
492
493 **RNA-Seq Analysis of Polysome Fractions.** Total RNA or pooled fractions from heavy
494 polysomes were isolated using Ribozol (Amresco) or Trizol (ThermoFisher) using standard
495 procedures, except the precipitant in the aqueous fraction was isolated using a RNeasy column
496 (Qiagen). mRNA was isolated from these total fractions using polyA enrichment (Dynabeads

497 mRNA DIRECT Micro Purification Kit, ThermoFisher) according to the manufacturers'
498 protocol, then library preparation was performed with Ion Total RNA-Seq Kit v2.0
499 (ThermoFisher). Library size, concentration, and quality was assessed using a 2200 TapeStation
500 (Agilent). Libraries were sequenced on Proton sequencer (ThermoFisher) with a PI chip and the
501 Ion PI Hi-Q Sequencing 200 Kit for 520 flows. Ion Torrent reads were processed using
502 combined Human Hg19 and KSHV (Accession GQ994935) reference transcriptomes. The
503 KSHV genome was manually re-annotated with the transcript definitions from KSHV2.0 (3)
504 reference transcriptome and the Quasi-Mapping software Salmon (88). Normalized counts per
505 million (cpm) were estimated for individual transcripts using the R package limma (89). Two
506 biological replicates were combined as a geometric mean (49). The transcripts were ordered by
507 abundance and the mean, standard deviation (SD), and Z-score were calculated using a sliding
508 window of 200 transcripts of similar abundance (49, 50). The most abundant 100 and the least
509 abundant 100 transcripts used the mean and SD of the adjacent bin. Translational efficiency (TE)
510 of a transcript treatment was determined by the formula TE = $\log_2$(polysome/total). The change
511 in translational efficiency (DTE) = TE_{Torin}-TE_{DMSO}.
512
513 **Polysome RT-qPCR.** TREx-BCBL1-RTA were reactivated with 1 µg/mL doxycycline for 24h.
514 Torin or DMSO was added two hours prior to harvest in high salt lysis buffer as described above.
515 Fractions were mixed 1:1 with Trizol and isolated as per manufacturer's directions except that
516 30-60 µg of GlycoBlue Co-Precipitant (Ambion) and 100 ng of *in vitro* transcribed luciferase
517 DNA (NEB T7 HiScribe) was added to the aqueous fractions during isopropanol precipitation
518 (52). The resulting pellet was resuspended in water and reverse transcribed with random primers
519 (Maxima H, ThermoFisher). mRNA was normalized to luciferase spike to control for recovery.
520 The quantity of mRNA detected in a given fraction was then calculated as a percentage of the
521 total detected in all fractions. The RNA recovery was controlled by subtracting the C_T of the
522 luciferase spike, which was assumed to be constant, from the target C_T. This ΔC_T value for each
523 fraction was then subtracted from the ΔC_T of the top fraction of the gradient to determine the
524 $\Delta\Delta C_T$. And transcript abundance (Q) was then calculated ($Q=2^{\Delta\Delta CT}$) for each fraction and all
525 fractions were summed. The total quantity of a transcript is represented as a proportion of the
526 total amount of detected transcript as per (52). Transcript quantities from the light, heavy, and
527 sub-polysomal fractions were grouped and summed for statistical analysis. Primer sequences are

528 listed in Table 1. Due to common usage of polyA signals and nesting of the viral genome, qRT-
529 PCR primers could amplify mRNA originating from more than one viral promoter (3). For
530 simplicity, PCR products are referred to by the mRNA coding region targeted by the primers.
531
532 **Polysome Western blot.** 500 µL fractions of sucrose gradient mixed with 45 µg of GlycoBlue
533 and 1.5 mL of 100% ethanol and incubated overnight at -80ºC. Fractions were centrifuged at
534 15,000 x *g* for 15 min at 4ºC. Supernatant was decanted and the pellet was washed 70% v/v
535 ethanol made with RNAase-free water. Residual ethanol was dried at 95ºC and the pellet was
536 resuspended in 1x Laemmli buffer with 100 mM DTT then boiled at 95ºC for 5 min prior to
537 SDS-PAGE.
538
539 **Gene Ontology Analysis.** Gene lists were searched for statistical over-representation for
540 molecular functions, using the PANTHER Classification System (www.pantherdb.org, (90)).
541 Lists were compared against the complete database using a Fisher's exact test, with a 1% FDR.
542 To determine enrichment of non-coding transcripts in the polysomes, transcripts were manually
543 sorted into coding and non-coding (NMD, lincRNA, retained-intron, processed pseudogenes, or
544 antisense transcripts) groups and compared using a Fisher's exact test, compared to all quantified
545 transcripts with a 1% FDR.
546
547 **shRNA gene silencing.** Lentiviruses derived from pLKO or pGIPZ were derived from
548 transfection of 293T cells with packaging plasmids pMD2.G and psPAX2 (gifts from Didier
549 Trono Addgene plasmids 12259 and 12260) using polyethylenimine MAX (polysciences
550 #24765). Lentiviruses were filtered at 0.45 µm before aliquoting and storage at -80ºC. TREx-
551 BCBL1-RTA cells were transduced with lentivirus overnight with 4 µg/mL polybrene
552 (hexadimethrine bromide, Sigma) and treated the following day with 1 µg/mL puromycin for a
553 further 2-3 d before seeding experiments. All experiments were seeded without puromycin.
554 shRNAs for eIF4E2, eIF4G2, and NCBP1 were selected from the GIPZ Lentiviral shRNA
555 library (ThermoFisher, sh-eIF4E2: V2LHS_68041; sh-eIF4G2 #1: V3LHS_323383, sh-eIF4G2
556 #2: V3LHS_323384; sh- NCBP1 #1: V3LHS_639361, sh-NCBP1 #2: V3LHS_645476). shRNA
557 sequences for METTL3 were selected from the RNAi Consortium (shMETTL3 - #1:
558 TRCN0000034715; shMETTL3 - #2: TRCN0000034714) and pLKO vectors were generated

559 according to the RNAi Consortium shRNA cloning protocol
560 (https://portals.broadinstitute.org/gpp/public/resources/protocols). A non-targeting shRNA
561 sequence was used as a control in all experiments, either pGIPZ-NS (ThermoFisher, RHS_4346),
562 or pLKO-NS-Puro, generated by replacing the BamHI/KpnI fragment of containing the
563 blasticidin selection cassette of pLKO-NS-BSD (a gift from Keith Mostov, Addgene plasmid
564 #26655 (91)) with the BamHI/KpnI-flanked puromycin selection cassette from pLKO-TRC (a
565 gift from David Root Addgene plasmid #10878 (92). Transduced cells were freshly generated for
566 every experiment and not maintained in culture for long periods. Knockdown was confirmed by
567 western blot after every lentivirus transduction.
568
569 **Viral replication.** DNAse-protected genomes were detected as described in (38). Briefly,
570 supernatant was treated with DNAse I (Sigma) for 30 min at 37°C to digest un-encapsidated
571 genomes. DNA was then harvested using DNeasy blood minikit (Qiagen) using buffer AL that
572 had been supplemented with salmon sperm DNA (Invitrogen) as carrier DNA and a luciferase-
573 encoding plasmid (pGL4.26, Promega). qPCR was then performed to detect viral gene ORF26
574 and luciferase from the carrier plasmid using *GoTaq* polymerase (Promega) and the $\Delta\Delta C_T$
575 method. Intracellular genomes were isolated from cells using DNeasy blood minikit and qPCR as
576 above.
577
578 **Statistics.** qRT-PCR values were calculated in Excel (Microsoft). Values were imported into
579 Prism8 (GraphPad) for statistical analysis and graphing. *P* values are represented in the figures
580 (*, $P < 0.05$; **, $P < 0.01$; ***, $P < 0.001$; ns, nonsignificant).
581
582 **Acknowledgments**
583 We thank members of the McCormick lab for critical discussion of this manuscript. We thank
584 Charles Craik (UCSF), Don Ganem (UCSF; Chang-Zuckerberg Biohub), S.-J. Gao (Pitt), David
585 Lukac (Rutgers), and Jae Jung (USC) for providing reagents.
586

587 **Table 1. Oligonucleotide sequences**

	Primer sequences (5'-3')	
qPCR Target	Forward	Reverse
luc2	TTCGGCAACCAGATCATCCC	TGCGCAAGAATAGCTCCTCC
Rps20	TTGACTTGCACAGTCCTTCTGA	ATGGTGACTTCCACCTCAAC
RACK1	GTGCTTCTGGAGGCAAGGAT	TCCCCACCATCTAGCGTGTA
β-actin	CTTCCAGCAGATGTGGATCA	AAAGCCATGCCAATCTCATC
LANA	TCCCACAGTGTTCACATCCG	GAGGTAAAGGTGTTGCGGGA
Kaposin	CACGTATCGAGGAGCGGTG	CAGGGTTCGCAGGGTTCG
VEGF-A	TTGTTGGAAGAAGCAGCCCA	AGGGGATGGAGGAAGGTCAA
hIL-6	TGCAATAACCACCCCTGACC	GTGCCCATGCTACATTTGCC
vIL-6	TCTCTTGCTGGTCGGTTCAC	CGGTACGGTAACAGAGGTCG
ORF11	ACATTTGACAACACGCACCG	AAAATCAGCACGCTCGAGGA
ORF45	TGATGAAATCGAGTGGGCGG	CTTAAGCCGCAAAGCAGTGG
ORF59	CACCAGGCTTCTCCTCTGTG	TCGCTGACAGACACAGTCAC
K8.1	AGATACGTCTGCCTCTGGGT	AAAGTCACGTGGGAGGTCAC
ORF26	CAGTTGAGCGTCCCAGATGA	GGAATACCAACAGGAGGCCG
ORF65	TGGCTCGCATGAATACCCTG	CTGCAGATGATCCCGCCTTT

588

589

590

591

592 **REFERENCES**
593

594 1. Jan E, Mohr I, Walsh D. 2016. A Cap-to-Tail Guide to mRNA Translation Strategies in
595 Virus-Infected Cells. Annu Rev Virol 3:283–307.
596 2. Glaunsinger BA. 2015. Modulation of the Translational Landscape During Herpesvirus
597 Infection. Annu Rev Virol 2:311–333.
598 3. Arias C, Weisburd B, Stern-Ginossar N, Mercier A, Madrid AS, Bellare P, Holdorf M,
599 Weissman JS, Ganem D. 2014. KSHV 2.0: a comprehensive annotation of the Kaposi's
600 sarcoma-associated herpesvirus genome using next-generation sequencing reveals novel
601 genomic and functional features. PLoS Pathog 10:e1003847.
602 4. Davis ZH, Hesser CR, Park J, Glaunsinger BA. 2015. Interaction between ORF24 and
603 ORF34 in the Kaposi's Sarcoma-Associated Herpesvirus Late Gene Transcription Factor
604 Complex Is Essential for Viral Late Gene Expression. J Virol 90:599–604.
605 5. Ye X, Zhaoid Y, Karijolich J. 2019. The landscape of transcription initiation across latent
606 and lytic KSHV genomes. PLoS Pathog 15:1–26.
607 6. Ganem D. 2010. KSHV and the pathogenesis of Kaposi sarcoma: listening to human
608 biology and medicine. J Clin Invest 120:939–949.
609 7. Boyne JR, Jackson BR, Taylor A, Macnab SA, Whitehouse A. 2010. Kaposi's
610 sarcoma-associated herpesvirus ORF57 protein interacts with PYM to enhance translation
611 of viral intronless mRNAs. EMBO J 29:1851–1864.
612 8. Sandri-Goldin RM. 2011. The many roles of the highly interactive HSV protein ICP27, a
613 key regulator of infection. Future Microbiol 6:1261–1277.
614 9. Sei E, Wang T, Hunter O V, Xie Y, Conrad NK. 2015. HITS-CLIP Analysis Uncovers a
615 Link between the Kaposi's Sarcoma-Associated Herpesvirus ORF57 Protein and Host
616 Pre-mRNA Metabolism. PLoS Pathog 11:e1004652.
617 10. Sharma NR, Majerciak V, Kruhlak MJ, Zheng Z-M. 2017. KSHV inhibits stress granule
618 formation by viral ORF57 blocking PKR activation. PLoS Pathog 13:e1006677.
619 11. Tan B, Liu H, Zhang S, da Silva SR, Zhang L, Meng J, Cui X, Yuan H, Sorel O, Zhang S-
620 W, Huang Y, Gao S-J. 2017. Viral and cellular N6-methyladenosine and N6,2′-O-
621 dimethyladenosine epitranscriptomes in the KSHV life cycle. Nat Microbiol 1–17.
622 12. Ye F, Chen ER, Nilsen TW. 2017. Kaposi's Sarcoma-Associated Herpesvirus Utilizes and
623 Manipulates RNA N6-Adenosine Methylation To Promote Lytic Replication. J Virol
624 91:JVI.00466-17.
625 13. Hesser CR, Karijolich J, Dominissini D, He C, Glaunsinger BA. 2018. N 6-
626 methyladenosine modification and the YTHDF2 reader protein play cell type specific
627 roles in lytic viral gene expression during Kaposi's sarcoma-associated herpesvirus
628 infection. PLoS Pathog 14:e1006995.
629 14. Baquero-Perez B, Agne A, Carr I, Whitehouse A. 2019. The Tudor SND1 protein is a
630 m6A RNA reader essential for KSHV replication. Elife 5:1–39.
631 15. Gilbert W V, Bell TA, Schaening C. 2016. Messenger RNA modifications: Form,
632 distribution, and function. Sci (New York, NY) 352:1408–1412.
633 16. Liu J, Yue Y, Han D, Wang X, Fu Y, Zhang L, Jia G, Yu M, Lu Z, Deng X, Dai Q, Chen
634 W, He C. 2013. A METTL3–METTL14 complex mediates mammalian nuclear RNA N6-
635 adenosine methylation. Nat Chem Biol 10:93–95.
636 17. Barbieri I, Tzelepis K, Pandolfini L, Shi J, Millán-Zambrano G, Robson SC, Aspris D,
637 Migliori V, Bannister AJ, Han N, De Braekeleer E, Ponstingl H, Hendrick A, Vakoc CR,

638 Vassiliou GS, Kouzarides T. 2017. Promoter-bound METTL3 maintains myeloid
639 leukaemia by m6A-dependent translation control. Nat Publ Gr 552:126–131.
640 18. Meyer KD, Patil DP, Zhou J, Zinoviev A, Skabkin MA, Elemento O, Pestova T V, Qian
641 S-B, Jaffrey SR. 2015. 5′ UTR m6A Promotes Cap-Independent Translation. Cell
642 1–13.
643 19. Coots RA, Liu X-M, Mao Y, Dong L, Zhou J, Wan J, Zhang X, Qian S-B. 2017. m6A
644 Facilitates eIF4F-Independent mRNA Translation. Mol Cell 68:504-514.e7.
645 20. Ries RJ, Zaccara S, Klein P, Olarerin-George A, Namkoong S, Pickering BF, Patil DP,
646 Kwak H, Lee JH, Jaffrey SR. 2019. m6A enhances the phase separation potential of
647 mRNA. Nature 1–23.
648 21. Mao Y, Dong L, Liu XM, Guo J, Ma H, Shen B, Qian SB. 2019. m6A in mRNA coding
649 regions promotes translation via the RNA helicase-containing YTHDC2. Nat Commun
650 10:1–11.
651 22. Liu N, Dai Q, Zheng G, He C, Parisien M, Pan T. 2015. N6 -methyladenosine-dependent
652 RNA structural switches regulate RNA-protein interactions. Nature 518:560–564.
653 23. Wang X, Zhao BS, Roundtree IA, Lu Z, Han D, Ma H, Weng X, Chen K, Shi H, He C.
654 2015. N6-methyladenosine Modulates Messenger RNA Translation Efficiency. Cell
655 161:1388–1399.
656 24. Dominissini D, Moshitch-Moshkovitz S, Salmon-Divon M, Amariglio N, Rechavi G.
657 2013. Transcriptome-wide mapping of N6-methyladenosine by m6A-seq based on
658 immunocapturing and massively parallel sequencing. Nat Protoc 8:176–189.
659 25. Thoreen CC, Chantranupong L, Keys HR, Wang T, Gray NS, Sabatini DM. 2012. A
660 unifying model for mTORC1-mediated regulation of mRNA translation. Nature 486:109–
661 113.
662 26. Hinnebusch AG. 2014. The Scanning Mechanism of Eukaryotic Translation Initiation.
663 Annu Rev Biochem 83:779–812.
664 27. Merrick WC. 2015. eIF4F: A Retrospective. J Biol Chem 290:24091–24099.
665 28. Pelletier J, Sonenberg N. 2019. The Organizing Principles of Eukaryotic Ribosome
666 Recruitment. Annu Rev Biochem 88:307–335.
667 29. Hsieh AC, Hsieh AC, Liu Y, Liu Y, Edlind MP, Edlind MP, Ingolia NT, Ingolia NT,
668 Janes MR, Janes MR, Sher A, Sher A, Shi EY, Shi EY, Stumpf CR, Stumpf CR,
669 Christensen C, Christensen C, Bonham MJ, Bonham MJ, Wang S, Wang S, Ren P, Ren P,
670 Martin M, Martin M, Jessen K, Jessen K, Feldman ME, Feldman ME, Weissman JS,
671 Weissman JS, Shokat KM, Shokat KM, Rommel C, Rommel C, Ruggero D, Ruggero D.
672 2012. The translational landscape of mTOR signalling steers cancer initiation and
673 metastasis. Nature 485:55–61.
674 30. Tcherkezian J, Cargnello M, Romeo Y, Huttlin EL, Lavoie G, Gygi SP, Roux PP. 2014.
675 Proteomic analysis of cap-dependent translation identifies LARP1 as a key regulator of
676 5'TOP mRNA translation. Genes Dev 28:357–371.
677 31. Lahr RM, Fonseca BD, Ciotti GE, Al-Ashtal HA, Jia J-J, Niklaus MR, Blagden SP, Alain
678 T, Berman AJ. 2017. La-related protein 1 (LARP1) binds the mRNA cap, blocking eIF4F
679 assembly on TOP mRNAs. Elife 6.
680 32. Philippe L, Vasseur J-J, Debart F, Thoreen CC. 2017. La-related protein 1 (LARP1)
681 repression of TOP mRNA translation is mediated through its cap-binding domain and
682 controlled by an adjacent regulatory region. Nucleic Acids Res.
683 33. Uniacke J, Holterman CE, Lachance G, Franovic A, Jacob MD, Fabian MR, Payette J,

684 Holcik M, Pause A, Lee S. 2013. An oxygen-regulated switch in the protein synthesis
685 machinery. Nature 486:126–129.
686 34. Maquat LE, Tarn W-Y, Isken O. 2010. The Pioneer Round of Translation: Features and
687 Functions. Cell 142:368–374.
688 35. Lee ASY, Kranzusch PJ, Doudna JA, Cate JHD. 2016. eIF3d is an mRNA cap-binding
689 protein that is required for specialized translation initiation. Nature 1–16.
690 36. Clippinger AJ, Maguire TG, Alwine JC. 2011. The Changing Role of mTOR Kinase in the
691 Maintenance of Protein Synthesis during Human Cytomegalovirus Infection. J Virol
692 85:3930–3939.
693 37. Walsh D, Perez C, Notary J, Mohr I. 2005. Regulation of the Translation Initiation Factor
694 eIF4F by Multiple Mechanisms in Human Cytomegalovirus-Infected Cells. J Virol
695 79:8057–8064.
696 38. Pringle ES, Robinson C-A, Mccormick C. 2019. KSHV lytic replication interferes with
697 mTORC1 regulation of autophagy and viral protein synthesis. J Virol.
698 39. Arias C, Walsh D, Harbell J, Wilson AC, Mohr I. 2009. Activation of Host Translational
699 Control Pathways by a Viral Developmental Switch. PLoS Pathog 5:e1000334.
700 40. Lenarcic EM, Ziehr B, De Leon G, Mitchell D, Moorman NJ. 2014. Differential Role for
701 Host Translation Factors in Host and Viral Protein Synthesis during Human
702 Cytomegalovirus Infection. J Virol 88:1473–1483.
703 41. McMahon R, Zaborowska I, Walsh D. 2010. Noncytotoxic Inhibition of Viral Infection
704 through eIF4F-Independent Suppression of Translation by 4EGi-1. J Virol 85:853–864.
705 42. Thoreen CC, Kang SA, Chang JW, Liu Q, Zhang J, Gao Y, Reichling LJ, Sim T, Sabatini
706 DM, Gray NS. 2009. An ATP-competitive Mammalian Target of Rapamycin Inhibitor
707 Reveals Rapamycin-resistant Functions of mTORC1. J Biol Chem 284:8023–8032.
708 43. Tabtieng T, Degterev A, Gaglia MM. 2018. Caspase-Dependent Suppression of Type I
709 Interferon Signaling Promotes Kaposi's Sarcoma-Associated Herpesvirus Lytic
710 Replication. J Virol 92.
711 44. Choe J, Lin S, Zhang W, Liu Q, Wang L, Ramirez-Moya J, Du P, Kim W, Tang S, Sliz P,
712 Santisteban P, George RE, Richards WG, Wong K-K, Locker N, Slack FJ, Gregory RI.
713 2018. mRNA circularization by METTL3–eIF3h enhances translation and promotes
714 oncogenesis. Nature 1–25.
715 45. Lin S, Choe J, Du P, Triboulet R, Gregory RI. 2016. The m6A Methyltransferase
716 METTL3 Promotes Translation in Human Cancer Cells. Mol Cell 62:335–345.
717 46. Sinclair NR. 2001. Fc-signalling in the modulation of immune responses by passive
718 antibody. Scand J Immunol 53:322–330.
719 47. Covarrubias S, Gaglia MM, Kumar GR, Wong W, Jackson AO, Glaunsinger BA. 2011.
720 Coordinated Destruction of Cellular Messages in Translation Complexes by the
721 Gammaherpesvirus Host Shutoff Factor and the Mammalian Exonuclease Xrn1. PLoS
722 Pathog 7:e1002339.
723 48. Davison AJ, Stow ND. 2005. New Genes from Old: Redeployment of dUTPase by
724 Herpesviruses. J Virol 79:12880–12892.
725 49. Quackenbush J. 2002. Microarray data normalization and transformation. Nat Genet
726 32:496–501.
727 50. Andreev DE, O'Connor PBF, Fahey C, Kenny EM, Terenin IM, Dmitriev SE, Cormican
728 P, Morris DW, Shatsky IN, Baranov P V. 2015. Translation of 5' leaders is pervasive in
729 genes resistant to eIF2 repression. Elife 4:e03971.

730 51. Joazeiro CAP. 2017. Ribosomal Stalling During Translation: Providing Substrates for
731 Ribosome-Associated Protein Quality Control. Annu Rev Cell Dev Biol 33:343–368.
732 52. Pringle ES, Mccormick C, Cheng Z. 2018. Polysome Profiling Analysis of mRNA and
733 Associated Proteins Engaged in Translation. Curr Protoc Mol Biol 125:e79.
734 53. Heyer EE, Moore MJ. 2016. Redefining the Translational Status of 80S Monosomes. Cell
735 164:757–769.
736 54. Sin SH, Roy D, Wang L, Staudt MR, Fakhari FD, Patel DD, Henry D, Harrington WJ,
737 Damania BA, Dittmer DP. 2007. Rapamycin is efficacious against primary effusion
738 lymphoma (PEL) cell lines in vivo by inhibiting autocrine signaling. Blood 109:2165–
739 2173.
740 55. Bais C, Santomasso B, Coso O, Arvanitakis L, Raaka EG, Gutkind JS, Asch AS,
741 Cesarman E, Gershengorn MC, Mesri EA, Gerhengorn MC. 1998. G-protein-coupled
742 receptor of Kaposi's sarcoma-associated herpesvirus is a viral oncogene and angiogenesis
743 activator. Nature 391:86–89.
744 56. Stallone G, Stallone G, Schena A, Schena A, Infante B, Infante B, Di Paolo S, Di Paolo S,
745 Loverre A, Loverre A, Maggio G, Maggio G, Ranieri E, Ranieri E, Gesualdo L, Gesualdo
746 L, Schena FP, Schena FP, Grandaliano G, Grandaliano G. 2005. Sirolimus for Kaposi's
747 sarcoma in renal-transplant recipients. N Engl J Med 352:1317–1323.
748 57. Liang Q, Chang B, Brulois KF, Castro K, Min CK, Rodgers MA, Shi M, Ge J, Feng P, Oh
749 BH, Jung JU. 2013. Kaposi's Sarcoma-Associated Herpesvirus K7 Modulates Rubicon-
750 Mediated Inhibition of Autophagosome Maturation. J Virol 87:12499–12503.
751 58. Lee J-S, Lee J-S, Li Q, Li Q, Lee J-Y, Lee J-Y, Lee SH, Lee SH, Jeong JH, Jeong JH, Lee
752 H-R, Lee H-R, Chang H, Chang H, Zhou F-C, Zhou F-C, Gao S-J, Gao S-J, Liang C,
753 Liang C, Jung JU, Jung JU. 2009. FLIP-mediated autophagy regulation in cell death
754 control. Nat Cell Biol 11:1355–1362.
755 59. Pattingre S, Pattingre S, Tassa A, Tassa A, Qu X, Qu X, Garuti R, Garuti R, Liang XH,
756 Liang XH, Mizushima N, Mizushima N, Packer M, Packer M, Schneider MD, Schneider
757 MD, Levine B, Levine B. 2005. Bcl-2 Antiapoptotic Proteins Inhibit Beclin 1-Dependent
758 Autophagy. Cell 122:927–939.
759 60. Satoh S, Hijikata M, Handa H, Shimotohno K. 1999. Caspase-mediated cleavage of
760 eukaryotic translation initiation factor subunit 2α. Biochem J 342:65–70.
761 61. Clemens MJ, Bushell M, Jeffrey IW, Pain VM, Morley SJ. 2000. Translation initiation
762 factor modifications and the regulation of protein synthesis in apoptotic cells. Cell Death
763 Differ 7:603–615.
764 62. Bushell M, Poncet D, Marissen WE, Flotow H, Lloyd RE, Clemens MJ, Morley SJ. 2000.
765 Cleavage of polypeptide chain initiation factor eIF4GI during apoptosis in lymphoma
766 cells: characterisation of an internal fragment generated by caspase-3-mediated cleavage.
767 Cell Death Differ 7:628–636.
768 63. Majerciak V, Kruhlak M, Dagur PK, McCoy J Philip J, Zheng Z-M. 2010. Caspase-7
769 Cleavage of Kaposi Sarcoma-associated Herpesvirus ORF57 Confers a Cellular Function
770 against Viral Lytic Gene Expression. J Biol Chem 285:11297–11307.
771 64. Henis-Korenblit S, Shani G, Sines T, Marash L, Shohat G, Kimchi A. 2002. The caspase-
772 cleaved DAP5 protein supports internal ribosome entry site-mediated translation of death
773 proteins. Proc Natl Acad Sci U S A 99:5400–5405.
774 65. Schmidt EK, Clavarino G, Ceppi M, Pierre P. 2009. SUnSET, a nonradioactive method to
775 monitor protein synthesis. Nat Methods 6:275–277.

776 66. Covarrubias S, Richner JM, Clyde K, Lee YJ, Glaunsinger BA. 2009. Host Shutoff Is a
777 Conserved Phenotype of Gammaherpesvirus Infection and Is Orchestrated Exclusively
778 from the Cytoplasm. J Virol 83:9554–9566.
779 67. Glaunsinger B, Ganem D. 2004. Highly Selective Escape from KSHV-mediated Host
780 mRNA Shutoff and Its Implications for Viral Pathogenesis. J Exp Med 200:391–398.
781 68. Belin S, Hacot S, Daudignon L, Therizols G, Pourpe S, Mertani HC, Rosa-Calatrava M,
782 Diaz J-J. 2010. Purification of ribosomes from human cell lines. Curr Protoc cell Biol
783 Chapter 3:Unit 3.40.
784 69. Mehta P, Woo P, Venkataraman K, Karzai AW. 2012. Ribosome purification approaches
785 for studying interactions of regulatory proteins and RNAs with the ribosome. Methods
786 Mol Biol 905:273–289.
787 70. Parra C, Ernlund A, Alard A, Ruggles K, Ueberheide B, Schneider RJ. 2018. A
788 widespread alternate form of cap-dependent mRNA translation initiation. Nat Commun 1–
789 9.
790 71. Castelli LM, Talavera D, Kershaw CJ, Mohammad-Qureshi SS, Costello JL, Rowe W,
791 Sims PFG, Grant CM, Hubbard SJ, Ashe MP, Pavitt GD. 2015. The 4E-BP Caf20p
792 Mediates Both eIF4E-Dependent and Independent Repression of Translation. PLOS Genet
793 11:e1005233.
794 72. Brugarolas J, Lei K, Hurley RL, Manning BD, Reiling JH, Hafen E, Witters LA, Ellisen
795 LW, Kaelin WG. 2004. Regulation of mTOR function in response to hypoxia by REDD1
796 and the TSC1/TSC2 tumor suppressor complex. Genes Dev 18:2893–2904.
797 73. Verma D, Li D-J, Krueger B, Renne R, Swaminathan S. 2015. Identification of the
798 physiological gene targets of the essential lytic replicative Kaposi's sarcoma-associated
799 herpesvirus ORF57 protein. J Virol 89:1688–1702.
800 74. Majerciak V, Uranishi H, Kruhlak M, Pilkington GR, Massimelli MJ, Bear J, Pavlakis
801 GN, Felber BK, Zheng ZM. 2011. Kaposi's Sarcoma-Associated Herpesvirus ORF57
802 Interacts with Cellular RNA Export Cofactors RBM15 and OTT3 To Promote Expression
803 of Viral ORF59. J Virol 85:1528–1540.
804 75. Izumiya Y, Kobayashi K, Kim KY, Pochampalli M, Izumiya C, Shevchenko B, Wang D-
805 H, Huerta SB, Martinez A, Campbell M, Kung H-J. 2013. Kaposi's Sarcoma-Associated
806 Herpesvirus K-Rta Exhibits SUMO-Targeting Ubiquitin Ligase (STUbL) Like Activity
807 and Is Essential for Viral Reactivation. PLoS Pathog 9:e1003506.
808 76. Du Y, Hou G, Zhang H, Dou J, He J, Guo Y, Li L, Chen R, Wang Y, Deng R, Huang J,
809 Jiang B, Xu M, Cheng J, Chen G-Q, Zhao X, Yu J. 2018. SUMOylation of the m6A-RNA
810 methyltransferase METTL3 modulates its function. Nucleic Acids Res 46:5195–5208.
811 77. Biever A, Glock C, Tushev G, Ciirdaeva E, Dalmay T, Langer JD, Schuman EM. 2020.
812 Monosomes actively translate synaptic mRNAs in neuronal processes. Science (80-) 367.
813 78. Sadler R, Wu L, Forghani B, Renne R, Zhong W, Herndier B, Ganem D. 1999. A complex
814 translational program generates multiple novel proteins from the latently expressed
815 kaposin (K12) locus of Kaposi's sarcoma-associated herpesvirus. J Virol 73:5722–5730.
816 79. Toptan T, Fonseca L, Kwun HJ, Chang Y, Moore PS. 2013. Complex Alternative
817 Cytoplasmic Protein Isoforms of the Kaposi's Sarcoma-Associated Herpesvirus Latency-
818 Associated Nuclear Antigen 1 Generated through Noncanonical Translation Initiation. J
819 Virol 87:2744–2755.
820 80. Gutierrez E, Shin B-S, Woolstenhulme CJ, Kim J-R, Saini P, Buskirk AR, Dever TE.
821 2013. eIF5A Promotes Translation of Polyproline Motifs. Mol Cell 51:35–45.

822 81. Rubio RM, Depledge DP, Bianco C, Thompson L, Mohr I. 2018. RNA m 6A modification
823 enzymes shape innate responses to DNA by regulating interferon β. Genes Dev 32:1472–
824 1484.
825 82. Winkler R, Gillis E, Lasman L, Safra M, Geula S, Soyris C, Nachshon A, Tai-Schmiedel
826 J, Friedman N, Le-Trilling VTK, Trilling M, Mandelboim M, Hanna JH, Schwartz S,
827 Stern-Ginossar N. 2018. m6A modification controls the innate immune response to
828 infection by targeting type I interferons. Nat Immunol 1–15.
829 83. Liu J, Dou X, Chen C, Chen C, Liu C, Michelle Xu M, Zhao S, Shen B, Gao Y, Han D,
830 He C. 2020. N6-methyladenosine of chromosome-associated regulatory RNA regulates
831 chromatin state and transcription. Science (80-) 367:580–586.
832 84. Larralde O, Smith RWP, Wilkie GS, Malik P, Gray NK, Clements JB. 2006. Direct
833 Stimulation of Translation by the Multifunctional Herpesvirus ICP27 Protein. J Virol
834 80:1588–1591.
835 85. Ricci EP, Mure F, Gruffat H, Decimo D, Medina-Palazon C, Ohlmann T, Manet E. 2009.
836 Translation of intronless RNAs is strongly stimulated by the Epstein–Barr virus mRNA
837 export factor EB2. Nucleic Acids Res 37:4932–4943.
838 86. Nakamura H, Lu M, Gwack Y, Souvlis J, Zeichner SL, Jung JU. 2003. Global changes in
839 Kaposi's sarcoma-associated virus gene expression patterns following expression of a
840 tetracycline-inducible Rta transactivator. J Virol 77:4205–4220.
841 87. Myoung J, Ganem D. 2011. Generation of a doxycycline-inducible KSHV producer cell
842 line of endothelial origin: maintenance of tight latency with efficient reactivation upon
843 induction. J Virol Methods 174:12–21.
844 88. Patro R, Duggal G, Love MI, Irizarry RA, Kingsford C. 2017. Salmon provides fast and
845 bias-aware quantification of transcript expression. Nat Methods 14:417–419.
846 89. Ritchie ME, Phipson B, Wu D, Hu Y, Law CW, Shi W, Smyth GK. 2015. limma powers
847 differential expression analyses for RNA-sequencing and microarray studies. Nucleic
848 Acids Res 43:e47–e47.
849 90. Mi H, Muruganujan A, Casagrande JT, Thomas PD. 2013. Large-scale gene function
850 analysis with the PANTHER classification system. Nat Protoc 8:1551–1566.
851 91. Bryant DM, Datta A, Rodríguez-Fraticelli AE, Peränen J, Martín-Belmonte F, Mostov
852 KE. 2010. A molecular network for de novo generation of the apical surface and lumen.
853 Nat Cell Biol 12:1035–1045.
854 92. Moffat J, Grueneberg DA, Yang X, Kim SY, Kloepfer AM, Hinkle G, Piqani B,
855 Eisenhaure TM, Luo B, Grenier JK, Carpenter AE, Foo SY, Stewart SA, Stockwell BR,
856 Hacohen N, Hahn WC, Lander ES, Sabatini DM, Root DE. 2006. A Lentiviral RNAi
857 Library for Human and Mouse Genes Applied to an Arrayed Viral High-Content Screen.
858 Cell 124:1283–1298.
859

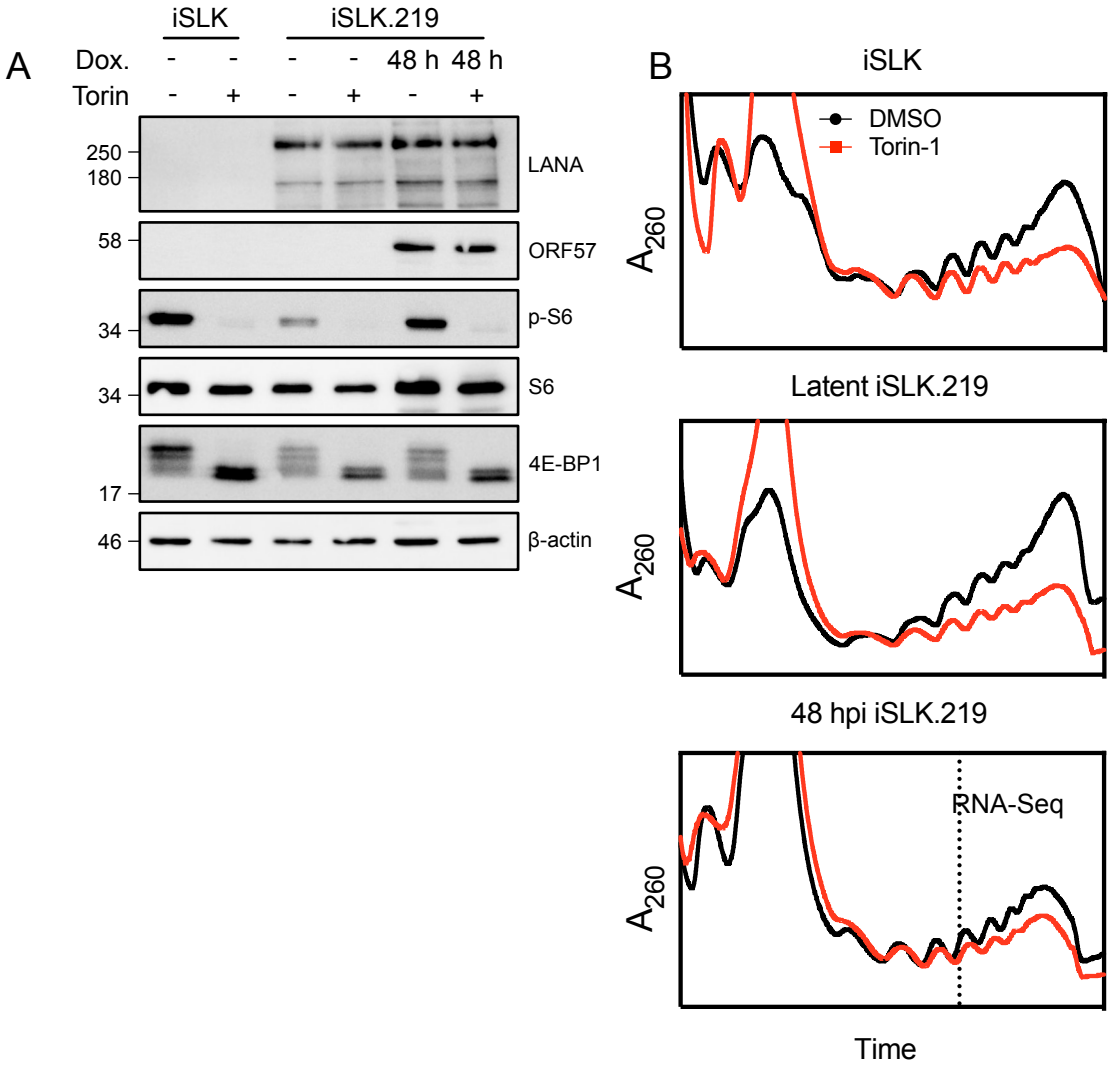

Fig 1. KSHV lytic replication reduces protein synthesis. (A) Western blots of whole cell lysates for polysome profiles. (B) Polysome profiles of uninfected, latent, or 48 hpi iSLK.219 treated with either Torin or DMSO for 2 h prior to harvest. Cells were treated with 100 µg/mL cycloheximide (CHX) for 5 minutes prior to harvest to prevent elongation. Cells were lysed in the presence of CHX and loaded on a 7-47% linear sucrose gradient. After separation by ultracentrifugation, the abundance of RNA (A_{260} nm) in the gradient was continually measure as fractions were collected. RNA from the 48 hpi polysome fractions was isolated for sequencing.

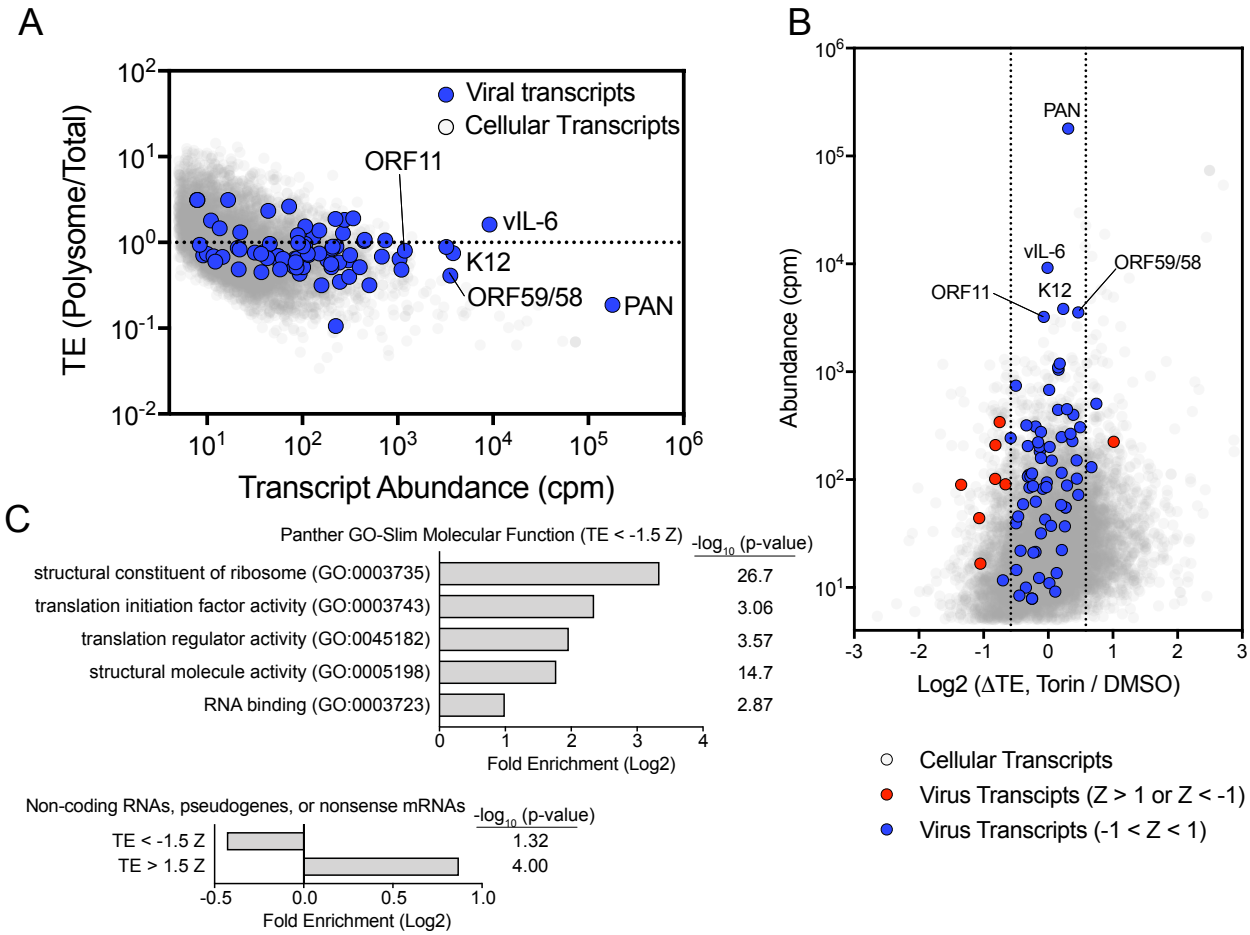

Fig 2. eIF4F disassembly does not affect translational efficiencies of viral mRNAs. mRNA from translating ribosomes (of DMSO treated cells) was sequenced and aligned to both the human and KSHV genomes. Viral transcripts are depicted in blue on top of the grey background of cellular genes. The dashed line represents the mean TE of all transcripts. (C) The Δ TE of viral transcripts is depicted in blue or red on a grey background of cellular genes. Viral transcripts beyond one SD of the mean are red, viral transcripts within on SD are depicted in blue. Vertical lines represent a 1.5-fold change in transcript TE. (D) Panther Gene Ontology-Slim molecular functions with a decreased TE during Torin treatment. (E) Depletion or enrichment of transcripts not predicted to encode functional proteins from TE < -1.5 Z or TE > 1.5 Z, respectively.

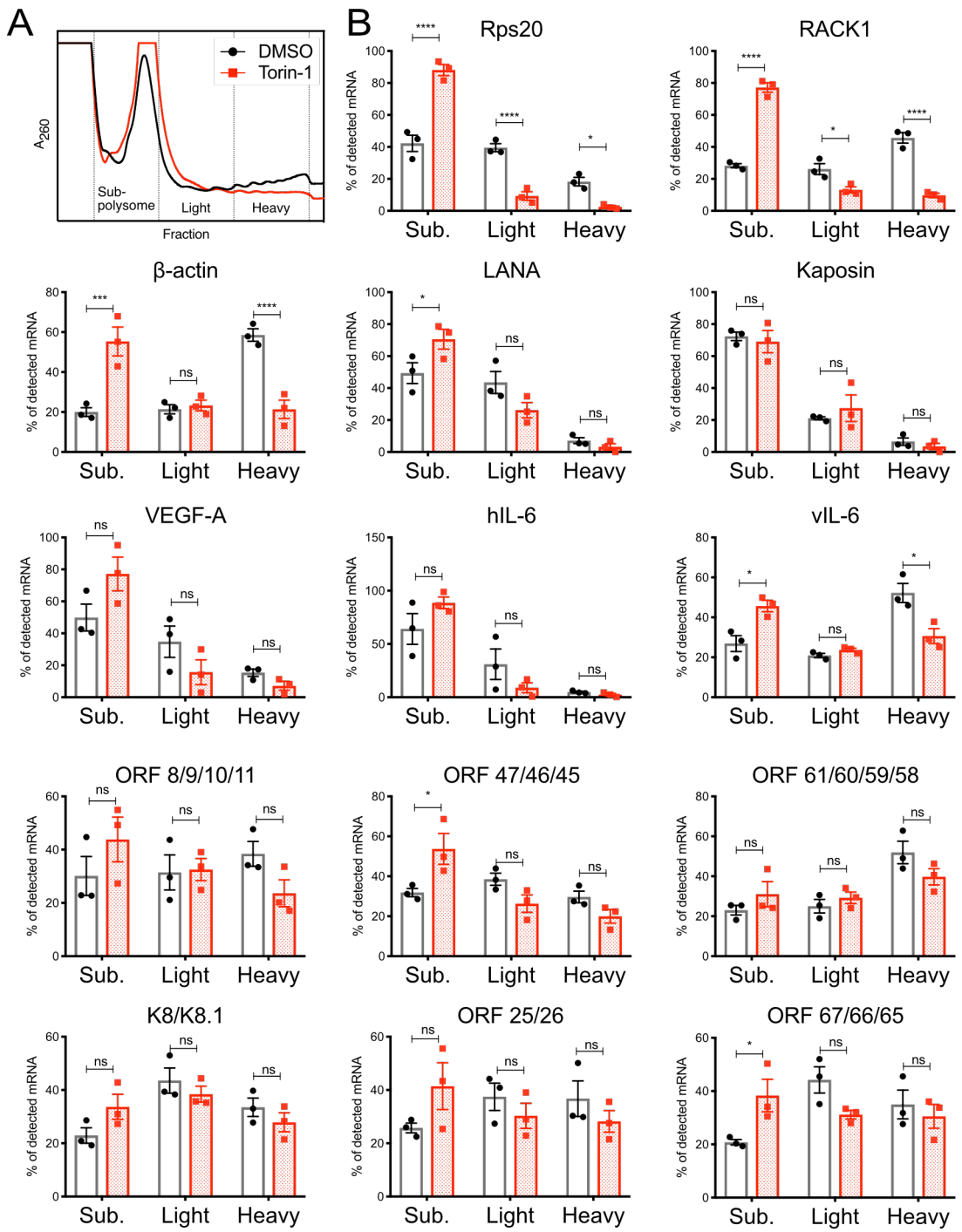

Fig 3. eIF4F disassembly does not deplete viral mRNAs from polysomes. (A) Polysome profile of TRex-BCBL1-RTA cells induced with 1 µg/mL dox for 24 h. Torin or DMSO control were added 2 h prior to harvest and polysome analysis. (B) qRT-PCR analysis of cellular and viral transcripts in polysome fractions. Total RNA was isolated from polysome fractions. RNA was co-precipitated with GlycoBlue and T7-transcribed luciferase RNA to improve and normalize for recovery. RNA was analysed by qRT-PCR for cellular, and viral transcripts. Vertical lines depict the boundaries between the monosomes, light polysome, and heavy polysome fractions (n=3; means±SEM; statistical significance was determined by two-way ANOVA).

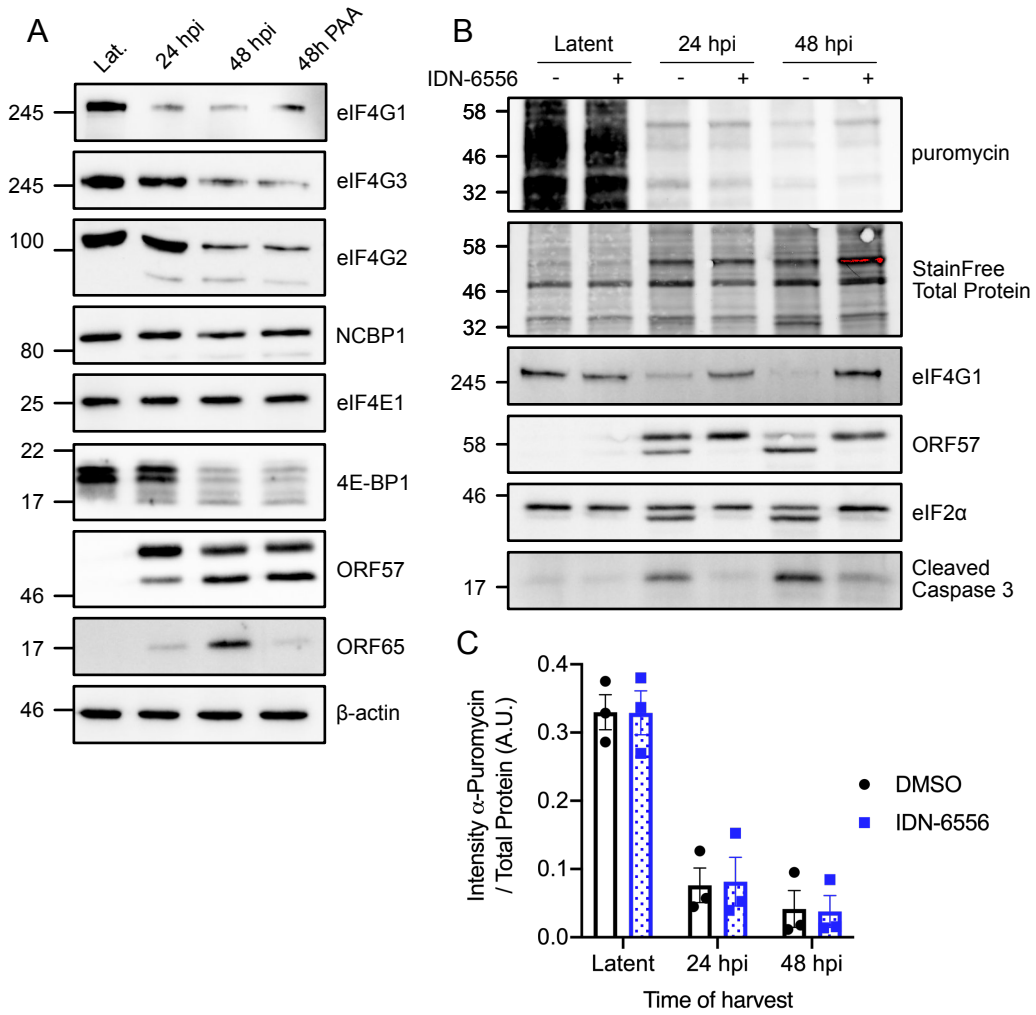

Fig 4. KSHV lytic replication reduces levels of host translation initiation factors (TIFs) but mTORC1 regulation of eIF4F formation remains intact. (A) TREx-BCBL1-RTA cells were treated with 1 µg/mL doxycycline. 500 µM PAA was added to inhibit genome replication as indicted. Cell lysate were probed by western blot as indicated. (B)TREx-BCBL1-RTA cells were reactivated as in (A). 10 µM IDN-6556 was added as indicated to inhibit caspases. 10 µg/mL of puromycin was added to all sample 10 minutes prior to harvest. (C) Quantification of puromycin blot relative to total protein amount(n=3; means±SEM; statistical significance was determined by two-way ANOVA).

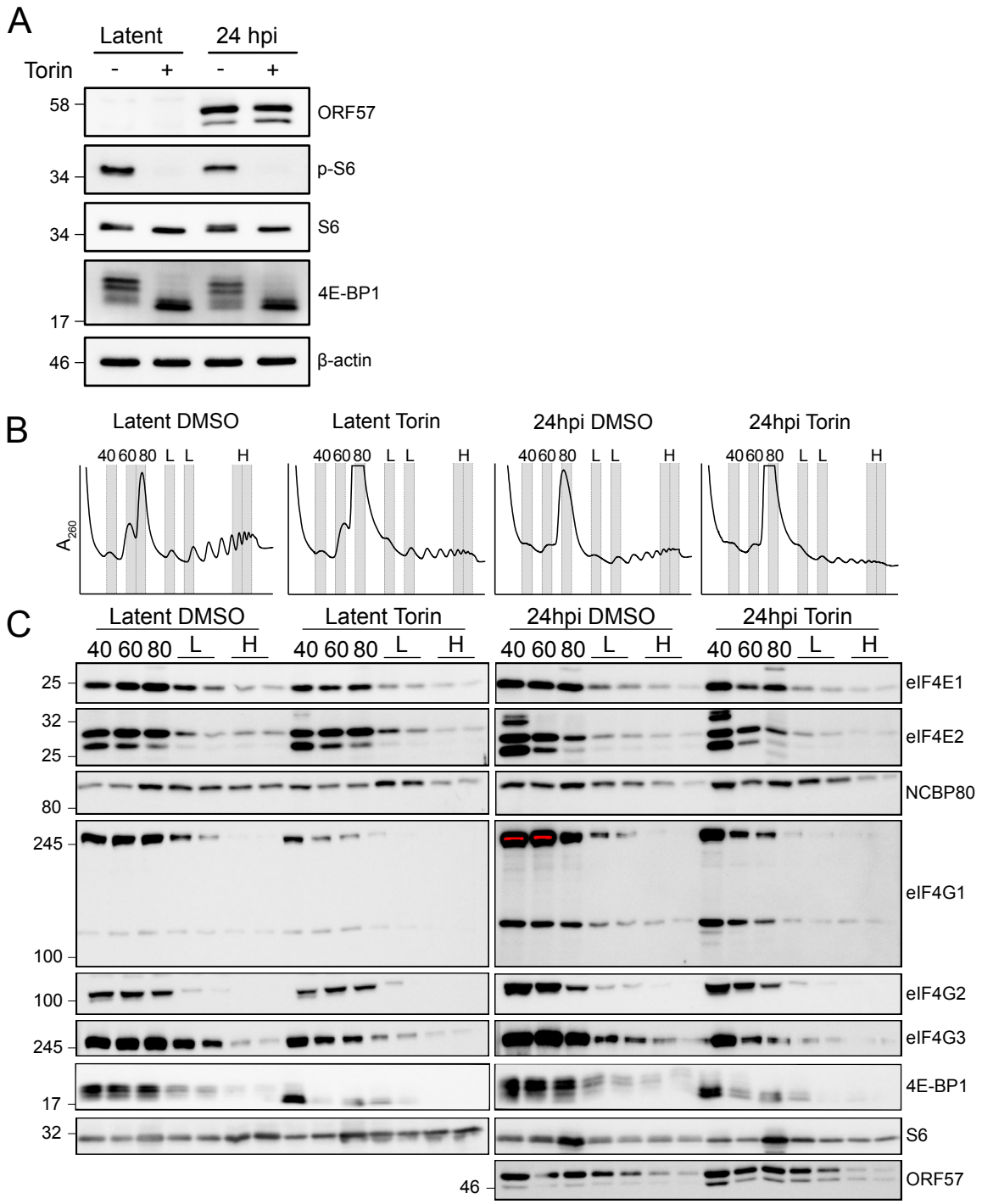

Fig 5. eIF4F disassembly selectively displaces host translation initiation factors from polysomes during KSHV latency and lytic replication. (A) Western blots of TREx-BCBL1-RTA whole cell lysates for polysome profiles. (B) Polysome profiles of TREx-BCBL1-RTA cells at 0 or 24 hpi, treated with Torin or DMSO control. Indicated 40S, 60S, 80S, light, and heavy polysome fractions were isolated for analysis. (C) Fractions were precipitated with glycogen and ethanol. The precipitate was resuspended in 1x Laemmli buffer and used for western blot analysis as indicated. Equal volume was loaded in all lanes.

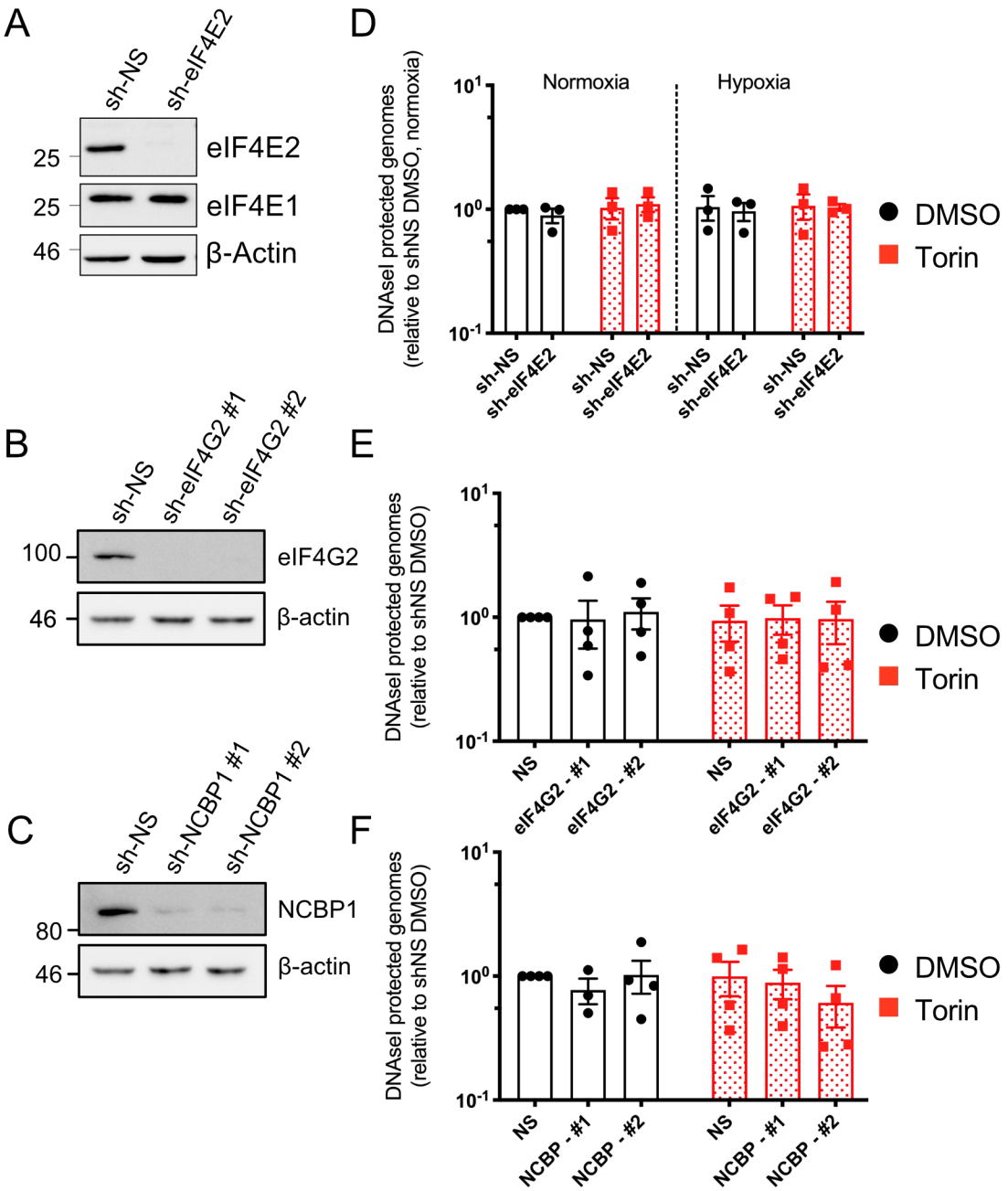

Fig. 6. KSHV virion production is unaffected by silencing of polysome-associated alternative translation initiation factors eIF4E2, eIF4G2 and NCBP1. (A-C) Knockdown of eIF4E2, NCBP1, or eIF4G2 in latent TREx-BCBL1-RTA cells. (D) eIF4E2 knockdown cells were reactivated with 1 µg/mL dox. At 24 hpi, cells were treated with DMSO or Torin, then either maintained in normal culture conditions, or were moved to a hypoxia chamber. Supernatant was harvested at 48hpi and processed for detection of DNase-protected genomes. (E-F) Reactivated TREx-BCBL-RTA cells were treated with DMSO or Torin at 24hpi. Supernatant was harvested at 48hpi and processed for detection of DNase-protected genomes (n=3-4; means±SEM; statistical significance was determined by two-way ANOVA).

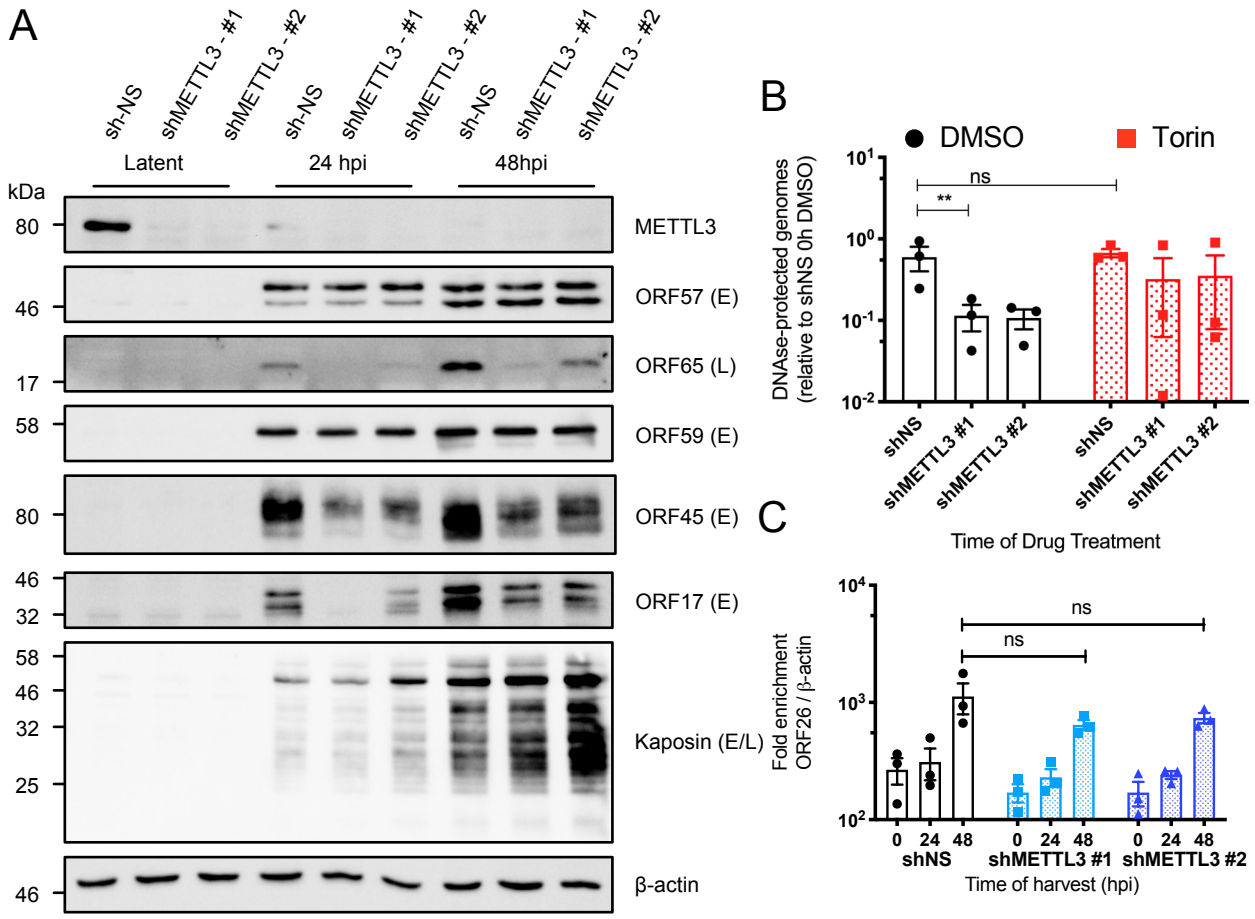

Fig. 7. The N6-methyladenosine methyltransferase METTL3 is required for efficient virion production but not genome replication (A) TREx-BCBL1-RTA cells were transduced with lentiviral shRNA constructs and selected with puromycin. Cells were reactivated with 1 µg/mL doxycycline and harvested as indicated. Lysates were probed for METTL3, early (E) proteins ORF57, ORF59 and ORF17 or late (L) proteins ORF65 or Kaposin. (B) Cells transduced and reactivated as in (A) were treated with DMSO or Torin at 0 or 24 hpi. Supernatant was harvested at 48hpi and processed for detection of DNase-protected genomes (n=3; means±SEM; statistical significance was determined by two-way ANOVA). (C) qPCR of intracellular viral genomes from DNA extracted from TREx-BCBL1-RTA cells treated as in (A) (n=3; means±SEM; statistical significance was determined by two-way ANOVA).

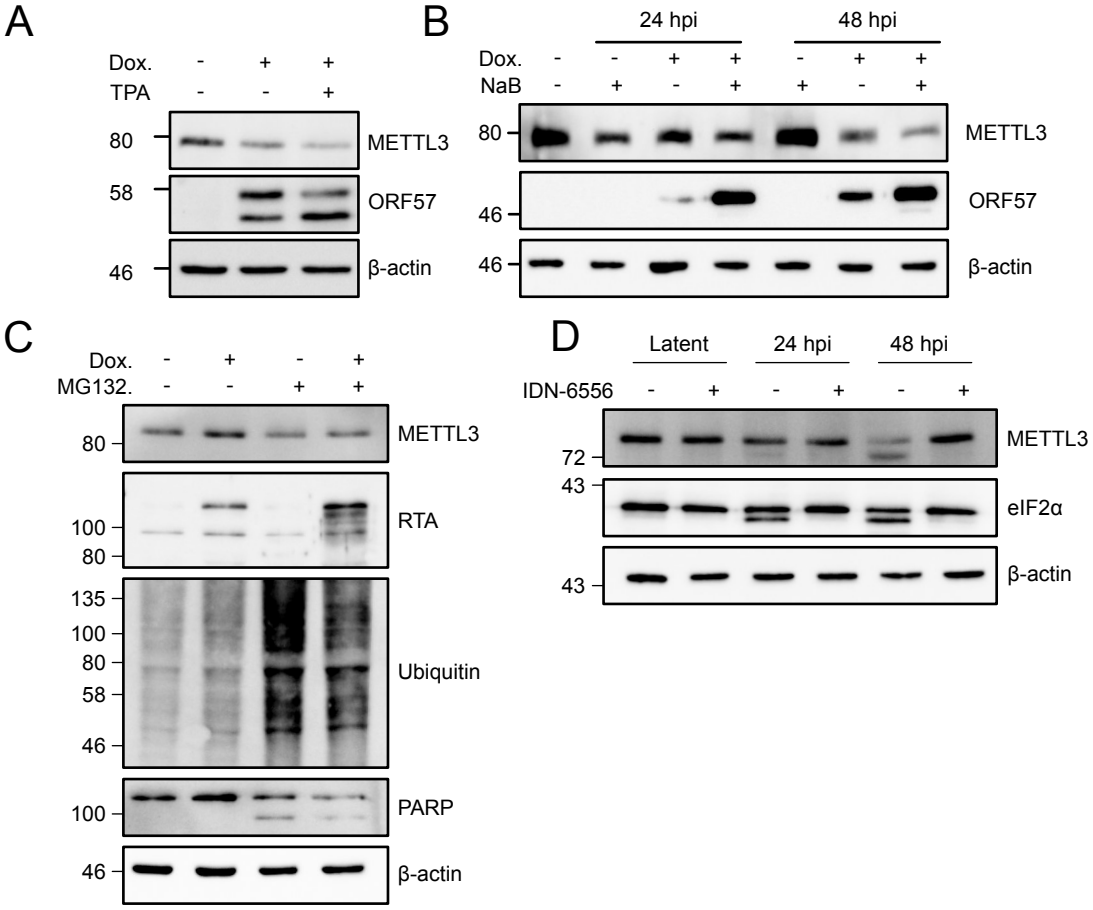

Fig. 8. METTL3 is degraded by caspase activity during lytic replication. (A) TREx-BCBL1-RTA cells were reactivated with 1 µg/mL dox in the presense of absence of 20 ng/mL 12-O-Tetradecanoylphorbol-13-acetate (TPA) and (B) iSLK.219 cells reactivated with 1 µg/mL dox in the presence of absence of sodium butyrate (NaB). METTL3 abundance was assessed by western blot. (C) Uninfected iSLK cells treated with 1 µg/mL dox to stimulate RTA expression were concurrently treated 10 µg/mL MG132 for 24 h and probed as indicated by western blot. (D) TREx-BCBL1-RTA cells treated with 1 µg/mL dox and 10 µM of IDN-6556 to inhibit caspases. Lysates were probed as indicated by western blot.